JPG Journal of Petroleum Geology www.jpg.co.uk

Journal of Petroleum Geology, Vol. 45(3), July 2022, pp 283-302

THE LA LUNA/RÍO NEGRO(.) PETROLEUM SYSTEM AT THE URDANETA WEST FIELD, LAKE MARACAIBO BASIN, NW VENEZUELA: 1D BASIN MODELLING AND SECONDARY OIL MIGRATION

M. Escobar[a,†], J.G. Díaz[b], G. Márquez[c,*], C. Boente[c] and R. Tocco[d]

This paper investigates the timing of hydrocarbon generation in the northern part of the Urdaneta West field in the NW of the Lake Maracaibo Basin, NW Venezuela, based on 1D basin modelling at three wells referred to as wells X, Y and Z. Kitchen areas were identified and secondary migration directions were inferred based on analyses of the thermal and burial history of the Upper Cretaceous La Luna Formation source rock and the geochemistry of 20 oil samples from the Río Negro Formation reservoir. Aliphatic hydrocarbons in the oil samples were analysed by gas chromatography – mass spectrometry (GC-MS) while the vanadium-nickel and sulphur contents were determined by energy dispersive X-ray spectrometry and inductively coupled plasma optical emission spectroscopy, respectively. Bulk and molecular characterizations indicated that the oils originated from a marine carbonate source rock containing oil-prone Type II kerogen, consistent with generation by the La Luna Formation.

Burial and thermal history modelling in the study area indicated that the La Luna source rock at wells X, Y and Z reached the oil window during the late Eocene, mid-Eocene and early Paleocene respectively. 1D model results from the three wells showed that hydrocarbon generation began in the early Eocene. The transformation ratio of the La Luna Formation source rock in the modelled wells reached values of 35%, 98% and 100% by the end of the Eocene.

In the Urdaneta West field, two different oil charges appear to have mixed in the Río Negro reservoir. Both oil charges were generated by the La Luna Formation source rock but at different times. A first charge of less mature oil occurred in the middle-late Eocene (Phase 1 generation), and a second, more mature oil charge took place in the Miocene – Quaternary (Phase 2 generation). The kitchen area for the first oil charge is inferred to have been located to the north and NE of Urdaneta West; that for the second oil charge to the south of the field. This migration model is supported by observed variations in the geochemical compositions of the oil samples analysed from different wells in the Urdaneta West field.

[a] School of Petroleum Geology, Faculty of Engineering, University of Zulia, Maracaibo 4002, Venezuela.
[b] PDVSA, Exploration and Production Activities, Av. 5 de Julio, Maracaibo, 4002, Venezuela.
[c] Center for Research in Sustainable Chemistry (CIQSO), University of Huelva, 21006 Huelva, Spain.
[d] Independent Petroleum Geochemistry Consultant, Madrid, 28410, Spain.
†deceased
* author for correspondence, email: gonzalo.marquez@diq.uhu.es

Key words: 1D basin model, petroleum geochemistry, reservoir-filling history, migration, source rock, La Luna Formation, Urdaneta West field, Lake Maracaibo Basin, Venezuela.

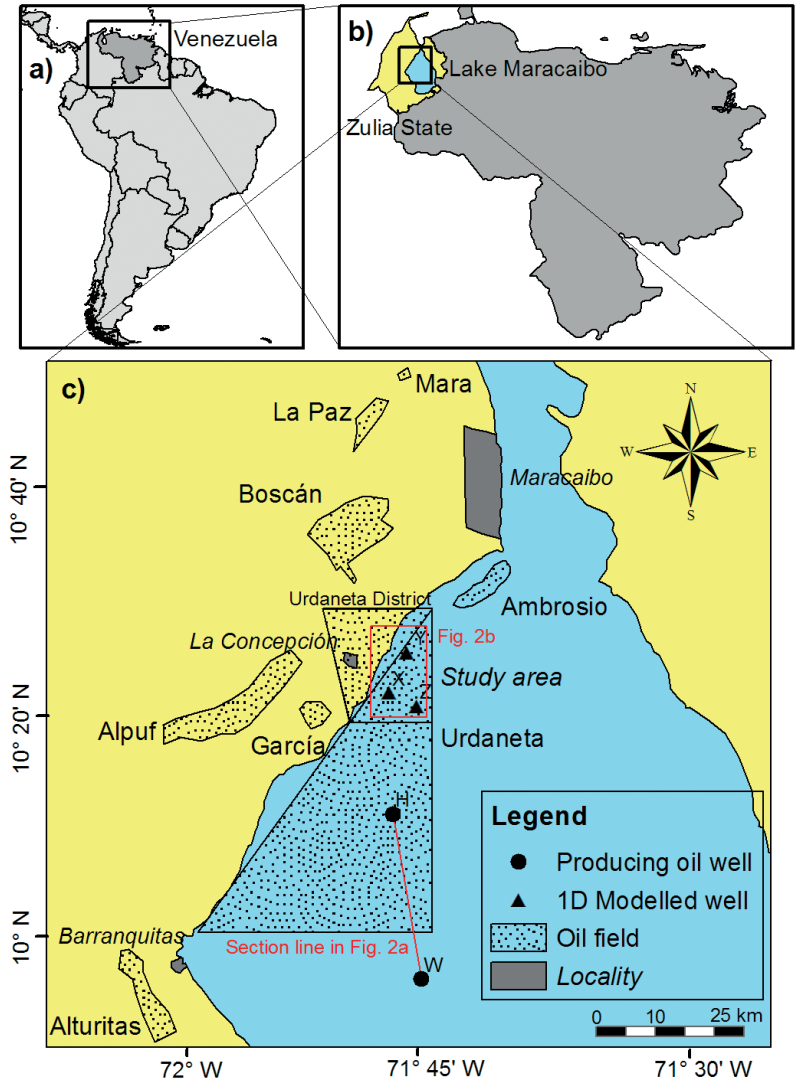

Fig. 1 (a, b). Maps showing the regional location of Lake Maracaibo in NW Venezuela. (c). Map shows the location of oilfields in the NW of Lake Maracaibo and adjacent onshore area, including Urdaneta West. The red box shows the study area in the offshore part of the field which is referred to as the Offshore Urdaneta District, and includes the locations of the three modelled wells (see Fig 2b). A cartoon section between wells H and W to the south of the study area is show in Fig. 2a.

INTRODUCTION

The Lake Maracaibo Basin in NW Venezuela (Fig. 1) covers an area of around 50,000 km^2 and has a sediment volume of approximately 250,000 km^3 (James, 2000). The basin extends over the present-day area of Lake Maracaibo (12,900 km^2) and parts of the adjacent hinterland. More than 17,000 oil wells have been drilled here in about 40 oilfields which are mostly located in Zulia State (Fig. 1B; Escobar *et al.*, 2011). The most important hydrocarbon source rock in the basin is the Cenomanian – Coniacian La Luna Formation (Talukdar *et al.*, 1986); less important source rocks include the Lower Cretaceous Machiques Member of the Apón Formation (Alberdi-Genolet and Tocco, 1999) and the Lisure Formation (Ascue, 2007). The main petroleum accumulations are found in fluvio-deltaic sandstones in the Eocene Misoa and Oligocene Icotea Formations together with the Miocene La Rosa and Lagunillas Formations (e.g. Sánchez, 2013). Although the Luna/Misoa (!) petroleum system accounts for 99% of the oil reserves in the Lake Maracaibo Basin (Talukdar and Marcano, 1994), other minor petroleum systems such as Marcelina/Misoa(.) and La Luna/Río Negro(.) have also been reported (Bracho, 2010; Escobar *et al.*, 2016) in the western part of the basin*.

A series of fields such as Alpuf, Alturitas, Ambrosio, Mara, Boscán, La Paz, Urdaneta West and García (Fig. 1C) produce oil from sandstones in the Misoa Formation and limestones in the Lisure and Maraca Formations of the Cretaceous Cogollo Group (Krause and James, 1990) (Fig. 2a). The Urdaneta West field,

* the symbols (.) and (!) denote hypothetical and proved petroleum systems, respectively (*sensu* Magoon and Dow, 1994)

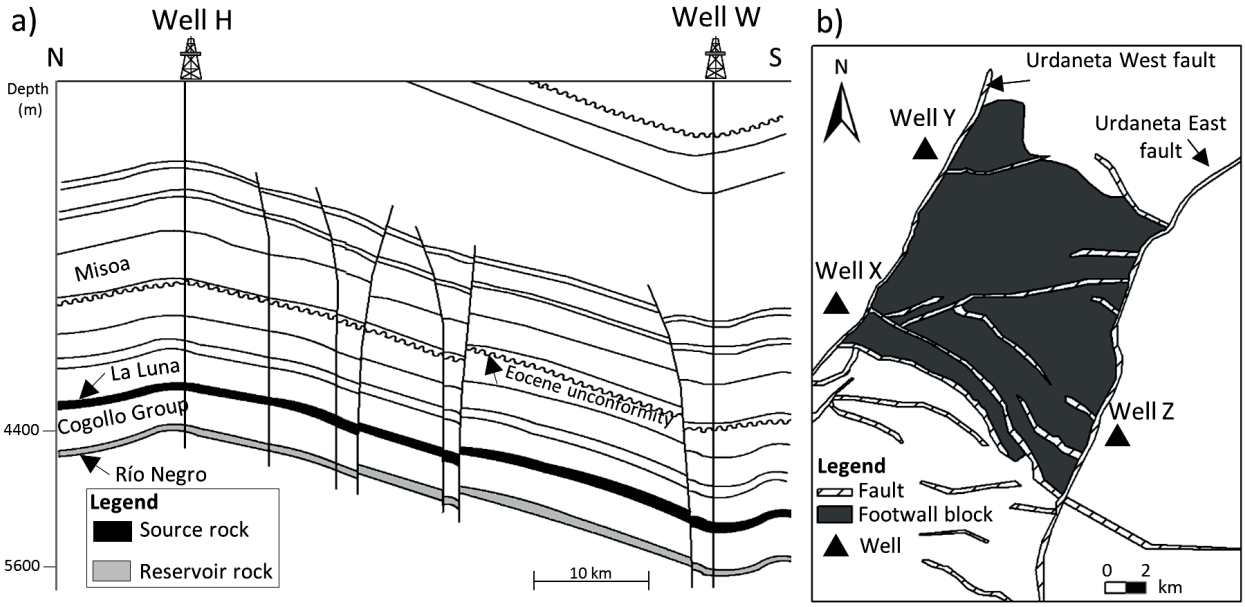

Fig. 2. (a) Schematic north-south cross-section between wells H and W in the southern part of the Urdaneta West field (profile line in Fig. 1c). (b) Outline structure map of the study area (see Fig. 1c for location).

the focus of this study, covers an area of 800 km^2 to the NE of the village of Barranquitas (Fig. 1C) and has reserves of about 1500 million barrels of oil (Talukdar and Marcano, 1994). Oil and gas is produced at 86 wells, mainly from the Misoa and Icotea Formations (Blaser and White, 1984); however there is some production from the Lower Cretaceous Río Negro sandstones (Sánchez, 2013). Initial exploration of the field was oriented towards the development of hydrocarbons in the "B" Sands of the Misoa Formation. However the need for new discoveries of proven oil and gas reserves has attracted considerable interest in the hydrocarbon potential of the Cretaceous succession, which is sealed above by the overpressured Colón Formation (Talukdar *et al.*, 1986) both at Urdaneta West and elsewhere in the western Lake Maracaibo Basin (Díaz, 2018; Montilla, 2018).

In this study, the thermal maturity and burial history of the La Luna Formation source rock, together with the timing of petroleum generation and expulsion, were modelled at three wells in the northernmost part of the Urdaneta West field in an area referred to as the "Offshore Urdaneta District" (wells X, Y and Z: locations in Fig. 1C). In addition, bulk geochemical and biomarker data for a set of oil samples from nearby wells were used to validate the one-dimensional basin model outcomes, and to provide information on the reservoir-filling history of the Urdaneta West field and the timing of the different phase(s) which have charged the Lower Cretaceous reservoir units there.

The aim of this paper is therefore to provide a broad understanding of the La Luna/Río Negro(.) petroleum system at the Urdaneta West field. Previous investigations of the La Luna Formation source rock (e.g. Blaser and White, 1984; Pérez-Infante *et al.*, 1996) are first reviewed. Then new data is presented for the studied petroleum system based on 1D numerical modelling of the La Luna source rock from three selected wells in the Offshore Urdaneta District and on geochemical analyses of oil samples from the Río Negro Formation in the Urdaneta West field. Finally, new information together with previously published data (Talukdar *et al.*, 1986; Talukdar and Marcano, 1994; Ascue, 2007; Díaz, 2018) is used to infer the location of kitchen areas and the direction of secondary oil migration into Lower Cretaceous reservoir sandstones at Urdaneta West.

Geological setting

The tectonic evolution of NW Venezuela (Lugo and Mann, 1995; Mann *et al.*, 2006) is constrained by the interaction of the North American, Caribbean and South American Plates (Macellari, 1988). Within this framework, numerous authors (e.g. Escalona and Mann, 2006) have divided the sedimentary column in the Lake Maracaibo Basin into various tectono-stratigraphic units (Fig. 3): (i) an Early to Late Cretaceous passive margin sequence; (ii) a transitional phase during the Cretaceous – Paleocene boundary interval, when the South American Plate was overridden as a result of collision with, and obduction of, the Pacific Plate volcanic arc and emplacement of the Lara nappes (a series of Lower to Upper Cretaceous igneous and metamorphic rocks overthrust onto the autochthon during the early Paleogene: Escalona and Mann, 2011); (iii) a Paleocene – Eocene foreland basin sequence which developed in front of the volcanic arc; and (iv) a late Eocene to Pleistocene sequence linked

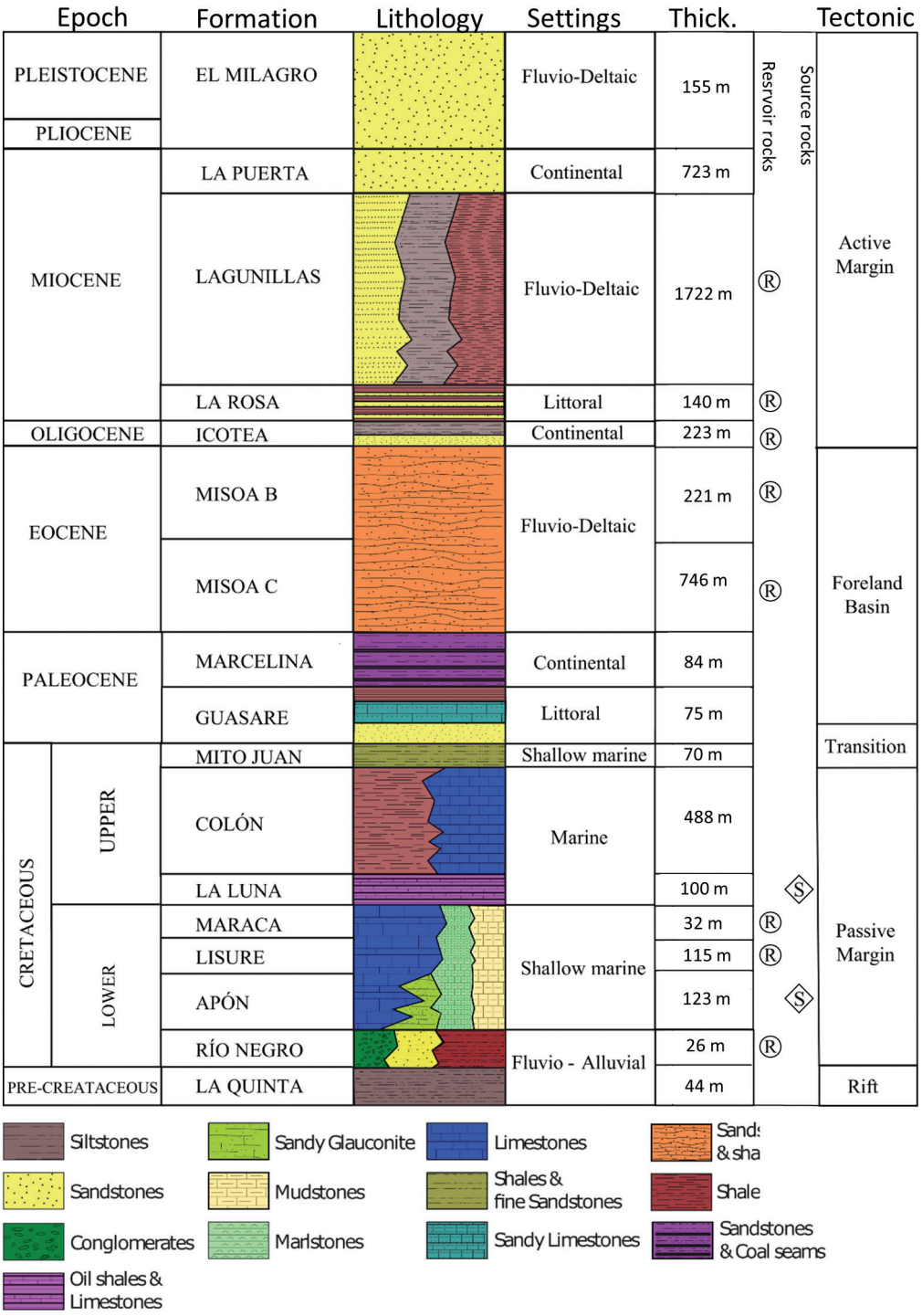

Fig. 3. Stratigraphic units in the Urdaneta West field (modified from Sánchez, 2013). Abbreviations: S, source rock; R, reservoir rock. The Apón, Lisure and Maraca Formations together form the Cogollo Group.

with the collision between the South American Plate and the Panama arc.

A series of mainly NE-SW and NW-SE oriented faults is present in the Offshore Urdaneta District (Fig. 2b), the most important of which are the Urdaneta West and Urdaneta East faults (Díaz, 2018). Unlike NW-SE oriented faults resulting from compressional stresses generated by the subduction zone at the NW margin of the South American Plate since Miocene time (Pöppelreiter *et al.*, 2005), the Urdaneta West and East faults formed as a result of extensional tectonics caused by the break-up of the American plate during the Jurassic (Villamil and Pindell, 1998) and bound rift grabens (Lugo and Mann, 1995). The former is a transpressional sinistral strike-slip fault oriented N45ºE; the latter, a N30ºE-oriented transpressional fault with left-lateral displacement which dips steeply towards the SE. These faults divide the Urdaneta

District into three blocks with different structural elevations (Fig. 2b); thus hangingwall blocks to the NW and SE are elevated compared with the central footwall block (Montilla, 2018). The hangingwall blocks consist of anticlines cut by the Urdaneta West and Urdaneta East faults, respectively. Likewise, the central (footwall) block consists of a SE dipping monocline affecting part of the Cretaceous succession, while the unconformably overlying Eocene succession dips to the SW (Pöppelreiter *et al.*, 2005) (Fig. 2a). This change in dip angle can be attributed to tilting of the basin due to the uplift of the Andean Cordillera and the Perijá Range during the Miocene (Guzmán and Fisher, 2006). These three structural blocks are cut by minor transverse faults that may act as migration baffles or barriers (Montilla, 2018).

Stratigraphy

The stratigraphic record at the Urdaneta West field comprises sedimentary rock units of Late Jurassic, Cretaceous and Cenozoic ages (Fig. 3; Talukdar *et al.*, 1986; Talukdar and Marcano, 1994; Sánchez, 2013; Díaz, 2018 among others). At the base of the section, the nearly 50 m thick La Quinta Formation consists of continental siltstones with igneous intrusions of Triassic to Jurassic age. Cretaceous sedimentation began with the deposition of continental clastics of the Berriasian – Hauterivian Río Negro Formation (arkosic sandstones and conglomerates interbedded with grey shales, < 30 m thick). The sandstones constitute important reservoir rocks. The overlying Cogollo Group, 270 m thick, was deposited during a marine transgression in the Early Cretaceous. The Group comprises the Barremian – lower Aptian Apón Formation (black and thin-bedded laminated limestones intercalated with black marlstones, dark mudstones, sandstones and sandy glauconitic shales); the upper Aptian – lower Albian Lisure Formation (sandy limestones and calcareous sandstones alternating with marlstones and grey shales); and the Albian Maraca Formation (fossiliferous sandy limestones, marlstones and grey shales). Limestones in the Cogollo Group are minor reservoir rocks.

The Cretaceous marine transgression reached its maximum extent during the Cenomanian – Coniacian with the deposition of the organic-rich black limestones and dark calcareous shales of the 100 m thick La Luna Formation (Cenomanian to early Campanian), which has TOC contents of up to 9.8 wt.% (average 3.8 wt.%). The La Luna Formation is in general mature to overmature and contains amorphous Type II kerogen. Hydrogen index values are up to 700 mg HC/g TOC at low levels of maturity (Blaser and White, 1984; Pérez *et al.*, 1996).

In the latest Cretaceous, the Campanian Colón Formation (limestones and calcareous shales almost 5000 m thick) and Maastrichtian Mito Juan Formation (60 m of dark shales and fine-grained calcareous sandstones) were deposited under relatively oxic (open marine) conditions. The Colón Formation acts as a regional seal.

The overlying Paleocene succession begins with shallow-marine and deltaic shales, calcareous sandstones and fine-grained sandy limestones of the 75 m thick Danian Guasare Formation, overlain by the Selandian to Thanetian Marcelina Formation (silty sandstones, siltstones and coals up to 84 m thick). Eocene sedimentation was mainly fluvio-deltaic with the deposition of the Misoa Formation (fine- to medium-grained sandstones intercalated with thin-bedded grey shales) with a thickness of ca. 1 km. The Misoa sandstones are the principal reservoir rocks in the basin. The Eocene sequence in Lake Maracaibo is confined between two regional unconformities: the "Paleocene unconformity", formed by erosion of the migrating forebulge created by tectonic loading as the Caribbean Plate approached western Venezuela; and the "Eocene unconformity", which was formed when tectonic loading moved eastward and the lithosphere responded by tectonic rebound (Escalona and Mann, 2006).

Overlying deposits comprise the non-marine silty sandstones and siltstones of the 223 m thick Icotea Formation (Rupelian and Chattian), followed in the earliest Miocene by the 140 m thick La Rosa Formation (shales and sandstones) and the Burdigalian – lower Tortonian Lagunillas Formation (fluvio-deltaic claystones, silts and sandstones), with a thickness of ca. 1700 m. Sandstones in the Icotea, La Rosa and Lagunillas Formations are also major reservoir rocks.

At the top of the sedimentary succession are continental sandstones and clays of the La Puerta Formation (725 m thick; upper Tortonian to Messinian) overlain by fluvio-deltaic, coarse-grained sandstones and claystones deposited during the Zanclean, and finally the 155 m thick El Milagro Formation.

Reservoir rocks

In the study area, the most important reservoir rocks occur in the Eocene Misoa Formation. The Misoa Formation can be divided into the "C" and "B" sandstones of Ypresian and Lutetian or later ages, respectively (Fig. 3) and these units can be further subdivided into 9 and 7 sub-units (Escobar *et al.*, 2016). The Misoa B sandstones are characterized by a higher proportion of laminated sandstones than those in the underlying C unit. Secondary reservoir rocks are present in the Lower Cretaceous Río Negro Formation and in the Miocene Icotea, La Rosa and Lagunillas Formations.

Porosities (12-28%, average 20%) and permeabilities (240 mD on average) of the Misoa

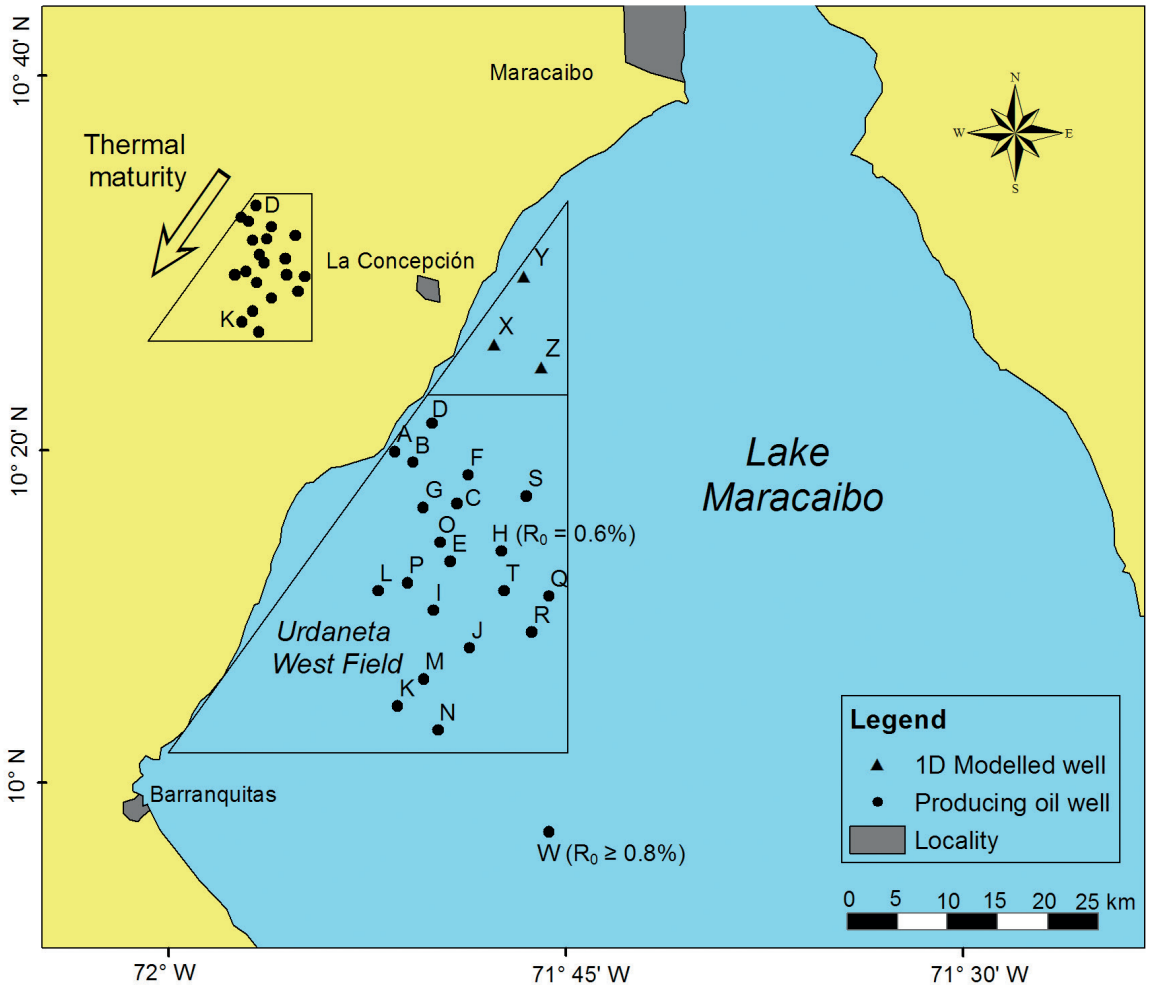

Fig. 4. Map of the study area in the NW Lake Maracaibo Basin showing the locations of the studied (modelled and producing) wells and the regional trend in oil maturity.

sandstones are higher than those in the Rio Negro sandstones (12-14% porosity and average 190 mD permeability). The Miocene La Rosa and Lagunillas sandstones have higher porosities (19-40%, average ~30%) and permeabilities (nearly 600 mD on average) than either of the underlying reservoir units (Talukdar and Marcano, 1994; Sánchez, 2013).

Petroleum system

Talukdar *et al.* (1986) recognized two main phases of oil and gas generation and expulsion from the La Luna Formation source rocks in the Lake Maracaibo Basin: mid-Eocene and Neogene-Quaternary. Significant burial of the formation occurred at the beginning of the Eocene, likely due to sediment deposition arising from the oblique collision of the Caribbean and South American Plates (Villamil, 1999). The main stage of petroleum generation and expulsion occurred during the mid-Eocene from a source kitchen in the NNE part of the basin. While the northern and NE parts of the basin were subsiding, the progressive generation of hydrocarbon fluids led to lower heat conductivities within the sedimentary column, and consequently the geothermal gradient decreases from NE to SW (Klemme, 1975). Moderate lateral variations in heat flow are therefore recorded both in the Offshore Urdaneta District (Díaz, 2018; see Fig. 6 below) and also in general throughout the entire basin (Talukdar *et al.*, 1986). Uplift of the basin during the Oligocene was accompanied by erosion and/or non-deposition, with the cessation of hydrocarbon generation and expulsion from the La Luna source rock. However important migration and entrapment processes occurred in late Eocene to early Miocene times (Lugo and Mann, 1995; Galarraga *et al.,* 2010).

Sediment deposition then resumed in the early Miocene in a foreland basin setting (Guzmán and Fisher, 2006), with increasing subsidence taking place in the Neogene – Quaternary in the south and SW of the basin ("Andean foredeep": Mann *et al.*, 2006). This subsidence was a consequence of the uplift of the Venezuelan Andes during the middle Miocene (Villamil, 1999) and coincided with a second phase of petroleum generation and expulsion from the La Luna source rock. The new source kitchens initially located in the south of the Lake Maracaibo Basin have progressively migrated towards the basin centre (Talukdar *et al.*, 1986).

Table 1. Stratigraphic sequences and corresponding tectonic events in the Lake Maracaibo Basin with estimates of average heat flow in mW/m² (Allen and Allen, 2005).

Sequence	Tectonic event	Mean heat flow
Jurassic	Extension	>85
Cretaceous	Passive margin	50
Late Cretaceous – Paleocene	Transition from passive to active margin	50-80
Late Paleocene – Post-Eocene	Collisional basins	70

Note: heat flow values expressed in mW/m^2.

SAMPLES AND METHODS

Modelling procedure

Three wells located in the Offshore Urdaneta District, referred to here as wells X, Y and Z (Fig. 1C, Fig. 4) were chosen to model hydrocarbon generation in, and expulsion from, the La Luna Formation source rock. The thermal and burial histories of the formation in the study area were assessed on the basis of the local stratigraphic column (Fig. 3) using BasinMod 1D software (Platte River Associates Inc.) following Peters *et al.* (2017) and Díaz (2018). The first stage in 1D basin modelling is the building of a conceptual geological model which is made up of continuous geological events with absolute ages (Ashrafi *et al.*, 2020; Mondal *et al.*, 2021). Petrophysical parameters such as porosity, density and thermal conductivity are calculated on the basis of lithological characteristics and the tools available in BasinMod. Palaeo surface and present-day temperature values are then used to calibrate the heat flow (Yalcin *et al.*, 1997).

Assessment of the quantity of hydrocarbons generated and expelled from the La Luna source rock was achieved on the basis of previously-defined inputs (e.g. geological events such as deposition or erosion, present day thicknesses/depths, and lithologies) from the three studied wells. Input data for numerical modelling include geochemical information such as original/present-day total organic carbon (TOC) contents and kerogen types (Díaz, 2018).

In order to define heat flow values, a qualitative reconstruction of the thermal history of the La Luna Formation was first carried out using heat flow estimates for various basin types (Table 1; Allen and Allen, 2005). Thermal maturities were calculated using the Basin%Ro model (Nielsen *et al.*, 2015). Phases of petroleum generation and expulsion were then determined assuming the presence of Type II kerogen in the source rock, an assumption supported by published stable carbon isotope data (Pérez-Infante *et al.*, 1996) and observations of amorphous marine organic matter which has high fluorescence under ultraviolet excitation (Talukdar *et al.*, 1986).

The numerical modelling followed a previous kinetic model of hydrocarbon generation and expulsion in the Maracaibo Basin which considered the geochemical characteristics of the La Luna Formation (Sweeney *et al.*, 1995), and used reaction kinetics based on the Burnham and Braun (1990) model.

Analytical methodologies

A set of 20 oil samples were collected from reservoir intervals in the Río Negro Formation at depths greater than 3500 m in the Urdaneta West field. The 20 sampled wells were located roughly 5 to 35 km south of the triangle delimited by wells X, Y and Z (Fig. 4; well locations in Table 2). Each oil sample was agitated in a batch reactor for 1 h at 60 ºC followed by a 12 h inactive period. According to the ASTM standard methodology, the asphaltenes were separated with *n*-heptane in a 1:40 v/v ratio using 0.45 μm filters and then treated several times by Soxhlet extraction with *n*-heptane until the liquid obtained by filtration turned colourless (Esquinas *et al.*, 2018). Maltenes were fractionated on activated alumina (Activity I, 80-200 mesh) into saturate, aromatic and resin fractions by liquid chromatography with *n*-hexane, toluene and dichloromethane:methanol (1:1, v/v), respectively.

Aliphatic hydrocarbons (paraffins) were analysed by gas chromatography – mass spectrometry (GC-MS) on a 7890A GC System coupled to a 5975C Inert XL MSD with a Triple-Axis Detector (Agilent Technologies). Gas chromatographic analyses were carried out on a DB-5ms capillary column (5% phenyl 95% dimethylpolysiloxane), 60 m × 0.25 mm i.d. × 0.10 μm film thickness from Agilent Technologies. Helium was used as a carrier gas. The oven temperature was initially set to 50 °C (held for 2 min), then ramped at 2.5 °C to 300 °C and held for 70 min. The mass spectrometer was calibrated daily with perfluorotributylamine under autotuning conditions, and the chromatograms were acquired in full-scan mode (mass range acquisition from *m/z* 45 to 500). The overall precision of the integrated areas under peaks in reconstructed mass chromatograms is 1-3 %.

From aliquots of each oil sample, the concentrations of vanadium and nickel were determined as well as the sulphur content following ASTM standard procedures, respectively, by means of an energy dispersive X-ray Panalytical spectrometer (Axios model) and a Perkin

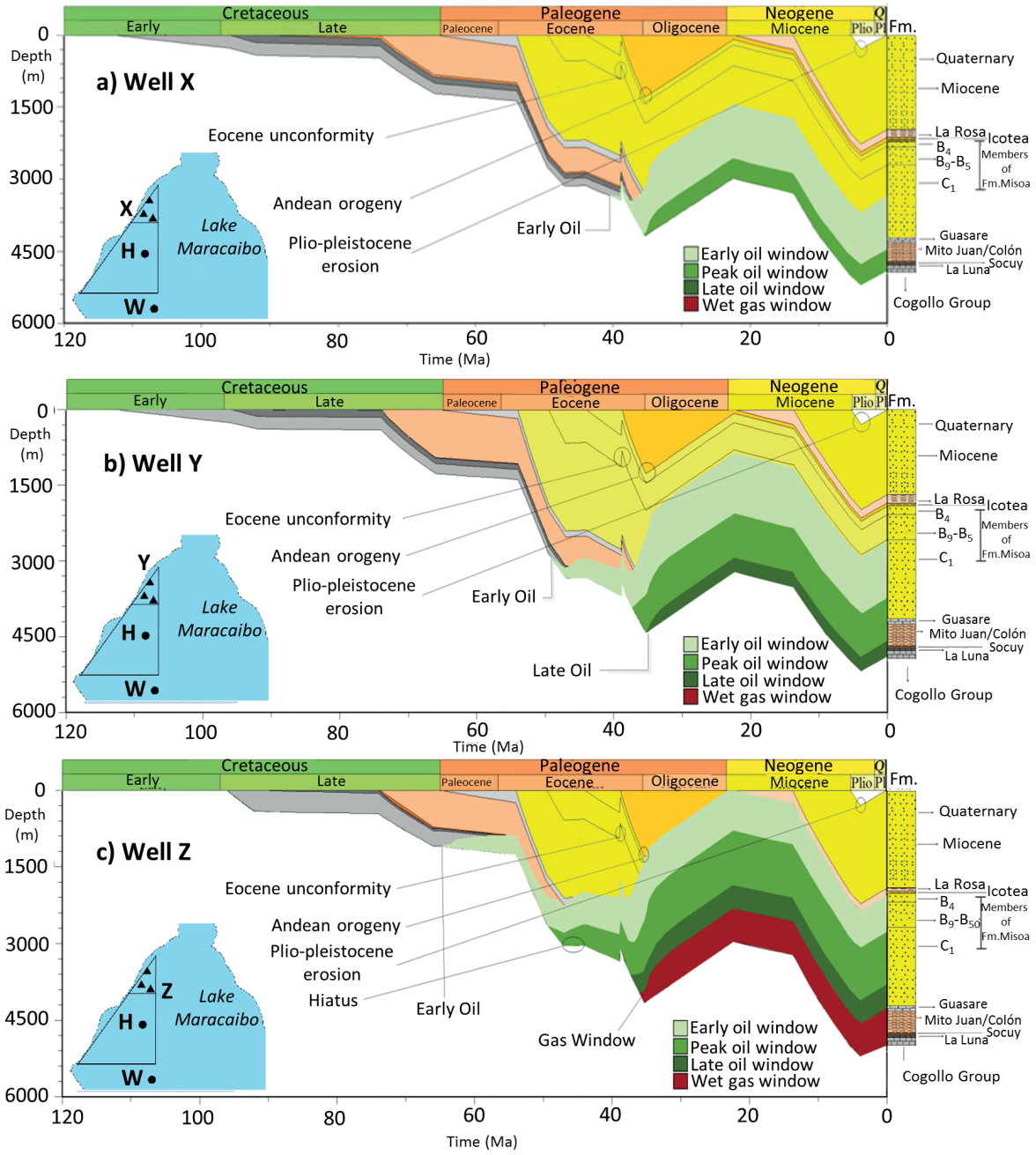

Fig. 5. Burial history curves with thermal maturation overlays (oil and gas windows) for modelled wells X (a), Y (b) and Z (c) in the Offshore Urdaneta District (well locations in Fig. 4).

Elmer Optima 3000 DV inductively coupled plasma optical emission spectroscopy (ICP-OES) system. In addition, the API gravity of each crude oil analysed was measured using the ASTM standard method. All analyses were conducted at Barcelona University.

RESULTS

1D basin modelling

Burial and thermal history modelling

The burial histories at wells X, Y and Z are in general similar (Fig. 5). Thus low rates of subsidence occurred during the pre-Maastrichtian Cretaceous (112-72 Ma) during the phase of passive margin sedimentation (Villamil, 1999). In the latest Cretaceous (72-66 Ma), the subsidence rate increased significantly to about 152 m per million years (m/Ma) corresponding to the transition from a passive margin to a retro-arc basin (Lugo and Mann, 1995). The Paleocene to earliest Eocene (65-52 Ma) was characterized by relatively low subsidence rates, but the subsidence rate increased significantly (up to about 455 m/Ma) during the early to middle Eocene (52-47 Ma) and again during the late Eocene (39-36 Ma). Subsequently, the Oligocene to earliest Miocene (35-23 Ma) was characterized

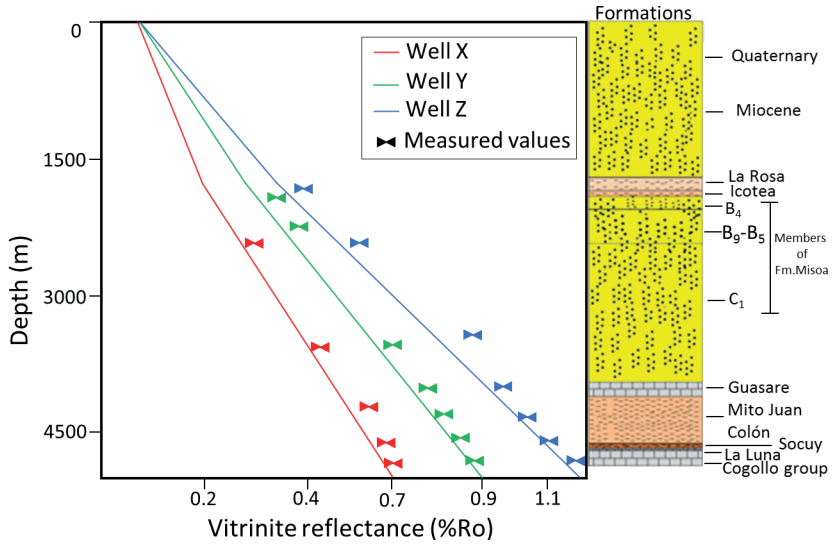

Fig. 6. Plots of measured (symbols) and calculated (lines) vitrinite reflectance versus depth for the three modelled wells (wells X, Y and Z) in the study area.

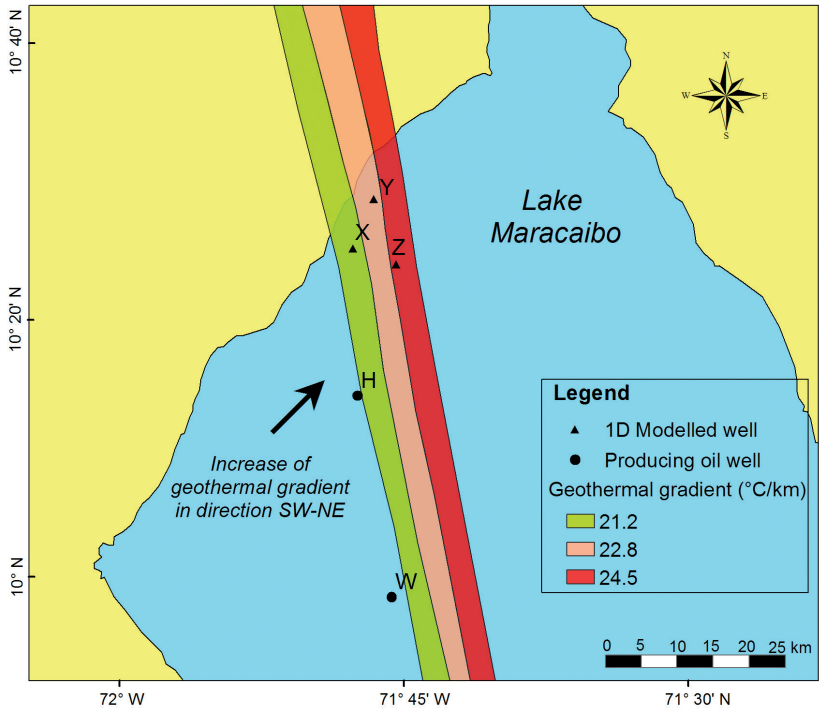

Fig. 7. Geothermal isogradient map for the NW Lake Maracaibo region and the Urdaneta West field.

by uplift at a rate of about 100 m/Ma. By contrast, the early to middle Miocene (23-14 Ma) and the late Miocene – Pliocene (14-4 Ma) were characterized by relatively high subsidence rates of about 30 and 167 m/Ma respectively. Finally, after the Cretaceous and Cenozoic succession in the three modelled wells had reached maximum burial depths during the Pliocene, uplift at a rate of about 60 m/Ma occurred and is continuing to the present day.

Previous studies of the tectonic events which governed the evolution of the centre-west of the Lake Maracaibo Basin (e.g. Pöppelreiter *et al.*, 2005; Mann *et al.*, 2006) were used to reconstruct the thermal history of the Urdaneta field area, which was calibrated with vitrinite reflectance (VR) data from Cretaceous and younger sediments from Díaz (2018). Calibration curves for the modelled wells X, Y and Z (Fig. 6) show that in general there is a good match between calculated (lines) and measured (symbols) VR data when plotted versus depth.

Heat flow values used for numerical modelling were adjusted using geothermal gradients determined from equilibrium temperatures at wells in the Urdaneta West field (Waples *et al.*, 1992; Díaz, 2018). The geothermal isogradient map for the study area (Fig. 7) shows heat flow values ranging from 21.2 to 24.5 °C/km (for a surface temperature of 27ºC), with values increasing from SW to NE. The calculated VR values

were determined using an algorithm from Nielsen *et al.* (2015) for the La Luna source rock at wells X, Y and Z, and are 0.6-0.7 $\%R_o$, 0.7-0.9 $\%R_o$ and 1.1-1.4 $\%R_o$ respectively. Assuming the maturity stages based on the Rock-Eval production index (PI) parameter, which is the ratio of free to total hydrocarbons within the source rock (Baskin, 1997), these values indicate present-day maturity levels which vary from the beginning of the oil window (0.55 to 0.7 $\%R_o$ and PI from 0.10 to 0.15), to the onset of the oil window (0.7 to 0.9 $\%R_o$ and PI from 0.15 to 0.25), and between the late oil window (< 1.35 $\%R_o$ and PI from 0.20 to 0.25) and the early dry gas generation stage (≥ 1.35 $\%R_o$ and PI < 0.20) respectively (c.f. Peters *et al.*, 2005).

Hydrocarbon generation, expulsion and accumulation

The timing of petroleum generation and expulsion from the La Luna source rock in the modelled wells was determined based on the thermal maturation history and assuming a Type II kerogen using the kinetic model given by Burnham and Braun (1990). The model results show that the La Luna source rock at wells X, Y and Z reached the oil window during the late Eocene, mid-Eocene and early Paleocene, respectively, at depths of around 3500 m, 3050 m and 1200 m (Fig. 5). Oil generation curves for these three wells (Fig. 8), i.e plots of the transformation ratio versus time (Yalcin *et al.*, 1997), indicate that significant (transformation ratios over 5%) hydrocarbon (mainly oil) generation from the La Luna Formation began during the Eocene at 35, 40 and 48 Ma respectively.

It can be interpreted from Fig. 8 that hydrocarbon generation from the La Luna source rocks in the Offshore Urdaneta District occurred almost entirely during Eocene to early Oligocene times. The transformation ratio (TR) for the La Luna Formation source rock at wells X, Y and Z during the early Oligocene (33-31 Ma) reached 35%, 98% and 100% (Fig. 8). The relatively low TR for the Eocene phase of oil generation from the La Luna Formation in well X, compared with the other modelled wells, could be explained by the location of the well. Well X is located in the hangingwall block to the SW of the Urdaneta West fault (Fig. 2b); at this location, the La Luna source rock only reached a relatively low level of thermal maturity (early oil window), as discussed above. Among other factors, this may have been because the geothermal gradient at this location is only 21.2ºC/km (Fig. 7).

The amounts of oil and gas generated per unit volume of source rock are related to the quantity, type and maturity of the kerogen present (Hakimi *et al.*, 2010). Amounts of oil and gas generated in the Offshore Urdaneta District were calculated based on the transformation ratio, the average source rock organic richness (TOC), and the Rock-Eval hydrogen index (HI) in the three modelled wells following the modelling methodology provided by Hantschel and Kauerauf (2009). During the Eocene – early Oligocene and for the assumed maturity model, the La Luna limestones and calcareous shales at wells X, Y and Z are modelled to have generated 66, 150 and 145 mg HC/g TOC oil, and 28, 23 and 65 mg HC/g TOC gas, respectively. During the Neogene – Quaternary, the calculated amounts of oil and gas generated by the La Luna source rock at the three wells were much lower: 12, 3 and 0 mg HC/g TOC, and 6, 3 and 25 mg HC/g TOC, respectively. Thus, although the La Luna Formation has been an effective hydrocarbon-generating source rock in the study area since the Eocene, most generation took place during the mid-Paleogene. These results are consistent with previous studies of the Cretaceous petroleum systems in this part of Lake Maracaibo Basin (Talukdar and Marcano; 1994; Pöppelreiter *et al.*, 2005).

An events chart for the La Luna/Río Negro(.) petroleum system in the centre-west of the Lake Maracaibo Basin was compiled based on the above modelling results and on previous publications (e.g. Díaz, 2018; Montilla, 2018) (Fig. 9). The chart shows that hydrocarbons originating from the Upper Cretaceous La Luna source rock migrated into the Lower Cretaceous Río Negro sandstones during Eocene to Oligocene and Neogene times. Modelling of the La Luna source rock in the study area suggests that hydrocarbon generation, migration and accumulation started in the Eocene and has continued until the present day. Fig. 9 identifies separate oil-generation phases 1 and 2. The La Luna source rock for the Urdaneta West field generated small volumes of oil from the mid-Oligocene onwards, in contrast to the La Luna kitchen located near the study area which reached the oil window in the Neogene (Talukdar *et al.*, 1986). The "critical moments" occurred in the mid-Miocene for phase 1 oils and the Holocene for phase 2.

Oil geochemistry

In order to validate the above modelling results, the geochemical characteristics of twenty oil samples from the Lower Cretaceous Río Negro Formation from wells in the Urdaneta West field were studied (well locations are shown in Fig. 4). Table 2 presents a list of the wells and the oil samples analysed together with API gravities and bulk geochemical information including the contents of asphaltenes (ASP), resins (RES) and aliphatic (saturated) and aromatic hydrocarbons (SAT, ARO).

Bulk geochemical data

The oil samples analysed have API values varying from 25º to 32º (Table 2). Their bulk compositions are

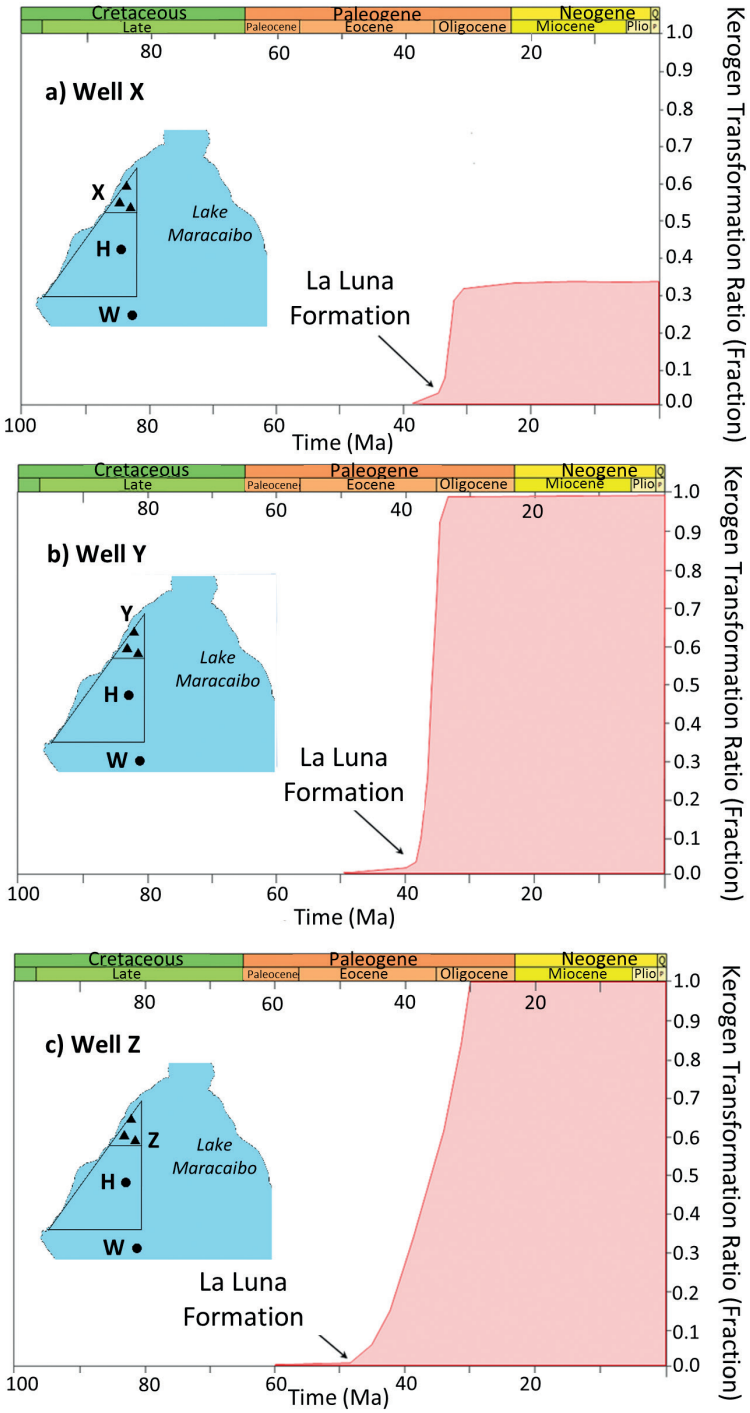

Fig. 8. Graphs showing the transformation ratio for the Upper Cretaceous La Luna source rock as a function of time in the modelled wells X (a),Y (b), and Z (c) in the Offshore Urdaneta District.

characterized by variable proportions of saturates (SAT), aromatics (ARO) and polar compounds (ASP+RES) (39-55%, 31-37% and 12-24%, respectively). These values are typical of non-biodegraded crude oils (Tissot and Welte, 1984). SARA fractionation showed that there is a close correlation (r^2 = 0.84) between the contents of asphaltenes and aromatics for the sampled oils, suggesting that the content of polar compounds does not appear to be due to the biodegradation of maltenes (Wenger *et al.*, 2002). The oil samples analysed exhibit relatively high sulphur contents, particularly those from wells in the northern part of the Urdaneta West field (Table 2). In general, there is an increase in sample API gravity from northeast to southwest: this could be consistent with the trend in the thermal maturity of the oils analysed, as discussed below.

V/(Ni+V) values >0.9, total sulphur contents > 1.5%, Ni concentrations below 90 ppm and V/Ni ratios >10 for the samples (Table 2, Figs 10a and 10b) suggest that the associated source rocks were deposited in a marine carbonate setting under anoxic conditions

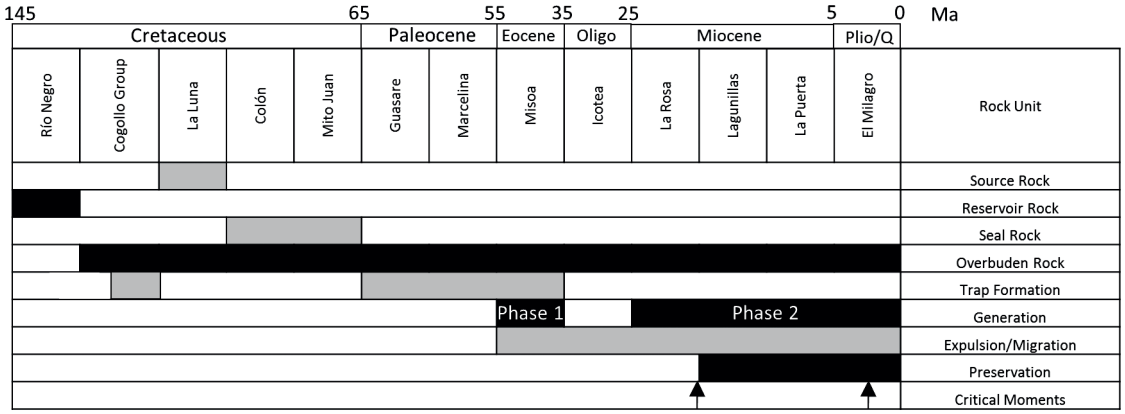

Fig. 9. Events chart for the La Luna/Río Negro(.) petroleum system in the NW of the Lake Maracaibo Basin showing key system elements and processes (generation, migration and accumulation).

(Lewan, 1984; Galarraga *et al*,, 2008). In sediments with relatively high sulphur contents (e.g. carbonates) deposited under anoxic conditions, bacterial sulphide is not completely sequestered by Fe ions. Ni ions will precipitate in metal sulphides rather than forming metal-organic compounds (porphyrins), contrasting with more stable V ions and resulting therefore in high V/Ni ratios. However, during deposition of shales (with low sulphur contents) under oxidizing conditions, Ni ions are more competitive for porphyrin metallation than V ions, which results in low V/Ni ratios (Lewan, 1984). In this latter case, sulphide ions are often removed by oxidation even if bacterial sulphide generation may also occur (Esquinas *et al.*, 2018). Although Ni and V contents can be affected by processes such as weathering and thermal maturation, the V/Ni ratio in a reservoired oil in general remains constant due to the similar structures and high thermal stabilities of the metal-organic compounds which contain both elements (Lewan and Maynard, 1982).

Molecular proxies and oil-source correlation

Total ion chromatograms for the analysed oil samples from the Río Negro Formation (e.g. Fig. 11a) show a unimodal pattern with a maximum below *n*-C_{22}, which is consistent with previous research indicating predominantly marine precursor organic matter (Bracho, 2010). Pristane-to-phytane ratios <0.89 for the sampled oils (Table 3) indicate that they were generated by source rocks deposited under anoxic conditions (c.f. Volkman and Maxwell, 1986). Although the relative abundances of these isoprenoids are controlled by a number of different processes (Dzou *et al.*, 1999), the Pr/Ph ratio can be used here to indicate the oxicity of the depositional environment. Fig. 10c shows a plot of Pr/*n*-C_{17} versus Ph/*n*-C_{18} for the oil samples (after Shanmugam, 1985) which can be interpreted to assess the redox conditions, depositional settings and type of the precursor organic material. The Pr/*n*-C_{17} ratio ≤ 0.5 and the Ph/*n*-C_{18} ratio > 0.3 (Table 3) suggest that the samples were generated from a marine carbonate source rock deposited under anoxic conditions.

Similarly, all the oil samples show very similar *m/z* 191 and 217 mass chromatograms (Figs. 11b and c; peak identifications are given in the Appendix: page 302). The samples are characterized by relatively high cheilanthane ratios (T/H), which could be explained by the thermal maturity (van Graas, 1990) rather than by biodegradation (Wenger *et al.*, 2002). C_{21}/C_{23} cheilanthane values < 1, low relative abundances of C_{24} 18β-de-E-hopane, C_{29}/C_{30} hopane ratios approaching or above 1, no predominance of C_{34} extended hopane over its C_{35} counterpart, and values of the ratio of Ts (18α-22,29,30-trisnorneohopane) to Tm (17α-22,29,30-trisnorhopane) lower than unity (Table 3, Fig. 11b) suggest that the analysed oils were generated from a carbonate source rock deposited in a reducing marine environment (c.f. Rullkötter *et al.*, 1985; Peters and Moldowan, 1991; Peters *et al.*, 2005). A marine carbonate source rock for the oils is in addition suggested by the distribution of C_{27}-C_{28}-C_{29} regular steranes (Fig. 11c), with a slightly higher relative abundance of C_{27} regular steranes in comparison to the C_{28} and C_{29} homologues; and also by the low relative abundances of diasteranes (Fig. 11c; Grantham and Wakefield, 1988; Van Kaam-Peters *et al.*, 1998).

Two main source rocks have been identified in the Lake Maracaibo Basin: the La Luna Formation (Cenomanian – Campanian) and the Machiques Member of the Apón Formation (Aptian – Albian). Saturated biomarker ratios for the La Luna and Machiques (Apón Formation) source rocks are shown in Table 3. Oil-source correlations were established by comparing data from the analyses of the oil samples from the Urdaneta West field with data previously reported for extracts of the La Luna and Apón source rocks (e.g. Talukdar *et al.*, 1986; Alberdi-Genolet and Tocco, 1999; Ascue, 2007). Taking into account

Table 2. List of wells studied ordered by location from north to south (locations in Fig. 4), together with oil sample API gravity, SARA percents, Ni concentrations (ppm), ratios of V/Ni and V/(Ni+V), and sulphur content (S, wt.%).

Well	Longitude	Latitude	°API	S	SAT	ARO	ASP	RES	Ni	V/Ni	V/(Ni+V)
Y	71º46'11''W	10º16'15''N	--	--	--	--	--	--	--	--	--
X	71º47'46''W	10º13'38''N	--	--	--	--	--	--	--	--	--
Z	71º43'00''W	10º10'27''N	--	--	--	--	--	--	--	--	--
D	71º50'38''W	10º08'43''N	25.3	2.30	39.5	37.5	9.1	13.9	28.4	10.2	0.91
A	71º54'58''W	10º07'08''N	25.1	2.29	40.1	37.3	7.6	15.0	31.8	11.0	0.92
B	71º52'35''W	10º06'32''N	25.7	2.20	40.0	37.7	8.1	14.2	30.1	12.8	0.93
F	71º48'59''W	10º06'05''N	25.5	2.23	41.2	37.1	7.8	13.9	26.0	11.1	0.92
S	71º46'04''W	10º05'22''N	25.7	2.25	40.4	36.8	7.8	15.0	29.8	11.6	0.92
C	71º49'42''W	10º04'16''N	25.8	2.34	39.7	35.6	8.0	16.7	35.2	13.0	0.93
O	71º51'07''W	10º03'47''N	26.1	2.27	40.2	35.7	6.7	17.5	39.9	11.4	0.92
G	71º50'25''W	10º02'17''N	26.9	2.20	43.5	37.5	6.0	13.0	33.2	13.8	0.93
H	71º47'39''W	10º02'14''N	27.5	2.10	41.5	35.9	6.4	16.2	35.3	11.1	0.92
E	71º50'29''W	09º59'49''N	28.0	1.92	44.7	34.0	5.2	16.1	29.5	10.4	0.91
P	71º52'43''W	09º59'39''N	28.7	1.89	47.3	32.2	5.6	14.9	20.9	13.2	0.93
Q	71º45'16''W	09º59'36''N	29.2	1.86	47.9	31.9	6.1	14.1	25.3	13.1	0.93
T	71º49'55''W	09º59'30''N	28.6	1.85	48.5	31.2	5.4	14.9	27.7	11.9	0.92
L	71º54'46''W	09º59'17''N	28.8	1.90	46.3	32.1	5.5	16.1	30.5	12.0	0.93
I	71º50'35''W	09º57'39''N	28.4	1.68	48.2	33.0	6.1	13.7	23.4	10.5	0.91
R	71º45'19''W	09º57'38''N	29.0	1.62	49.4	32.4	5.1	13.1	22.5	10.7	0.91
J	71º48'39''W	09º56'00''N	30.6	1.51	50.1	32.0	5.5	12.4	20.6	12.1	0.93
M	71º51'08''W	09º54'13''N	31.9	1.52	53.8	30.8	4.0	10.4	37.1	12.6	0.93
K	71º51'11''W	09º54'07''N	32.0	1.49	54.9	31.0	4.7	9.4	32.0	11.2	0.92
N	71º50'26''W	09º52'00''N	32.2	1.56	55.0	32.3	4.6	8.1	39.1	10.3	0.91
W	71º42'57''W	09º43'31''N	--	--	--	--	--	--	--	--	--

Notes: SAT=saturates; ARO=aromatics; RES=resins; and ASP=asphaltenes

Table 3. Source- and maturity-related molecular parameters for saturates in oil samples and source rocks analysed.

Sample	Pr/Ph	Pr/*n*-C_{17}	Ph/*n*-C_{18}	Ts/Tm	29/30H	21/23T	24Tet/23T	T/H	%20S	%ββ
Oil D	0.71	0.50	0.75	0.32	1.16	0.24	0.13	0.69	49	51
Oil A	0.77	0.45	0.73	0.34	1.00	0.27	0.13	0.76	48	51
Oil B	0.86	0.44	0.70	0.35	1.18	0.24	0.10	0.99	48	50
Oil F	0.73	0.53	0.72	0.34	1.11	0.27	0.13	0.76	48	51
Oil S	0.66	0.51	0.76	0.35	1.03	0.25	0.11	0.80	47	50
Oil C	0.59	0.53	0.89	0.37	1.18	0.25	0.12	0.85	47	51
Oil O	0.73	0.47	0.84	0.36	1.09	0.23	0.10	0.88	48	52
Oil G	0.71	0.50	0.75	0.35	1.15	0.29	0.11	0.75	48	52
Oil H	0.68	0.40	0.80	0.30	1.06	0.30	0.11	1.03	47	53
Oil E	0.70	0.48	0.80	0.38	1.10	0.27	0.12	1.02	49	52
Oil P	0.71	0.49	0.69	0.40	1.10	0.28	0.12	0.97	50	53
Oil Q	0.74	0.46	0.71	0.42	1.04	0.23	0.11	1.01	50	54
Oil T	0.70	0.55	0.75	0.45	1.05	0.26	0.10	1.02	50	56
Oil L	0.65	0.39	0.70	0.48	1.03	0.31	0.12	1.13	51	55
Oil I	0.72	0.56	0.72	0.50	1.02	0.27	0.11	1.15	52	56
Oil R	0.74	0.46	0.78	0.51	1.07	0.26	0.12	1.24	52	58
Oil J	0.69	0.54	0.80	0.53	0.99	0.25	0.13	1.29	54	61
Oil M	0.78	0.52	0.78	0.58	1.11	0.25	0.12	1.35	53	60
Oil K	0.89	0.53	0.79	0.60	1.04	0.28	0.11	1.30	54	61
Oil N	0.69	0.50	0.81	0.63	0.97	0.30	0.12	1.25	54	62
La Luna	0.67	0.44	0.68	0.49	1.24	0.29	0.14	0.73	39-55	25-63
Apón	1.15	1.00	1.05	11.50	0.50	0.69	0.16	0.63	43	58

Notes: Pr/Ph=pristane/phytane; Pr/*n*C_{17}=pristane/*n*-heptadecane; Ph/*n*C_{18}=phytane/*n*-octadecane; Ts/Tm=18α(H)-22,29,30-trisnorneohopane/17α(H)-22,29,30-trisnorhopane; 29/30H=30-norhopane/hopane; 21/23T=C_{21}-tricyclic terpane/C_{23}-tricyclopolyprenane; 24Tet/23T= C_{24}-tetracyclic terpane/C_{23}-cheilanthane; T/H=ratio of cheilanthanes to hopanes; %20*S*=5α,14α,17α(H)-stigmastane 20S and 20R ratio (%); and %ββ=ratio (%) of C_{29} isosteranes (20*S*+20*R*) to C_{29} regular steranes (20*S*+20*R*).

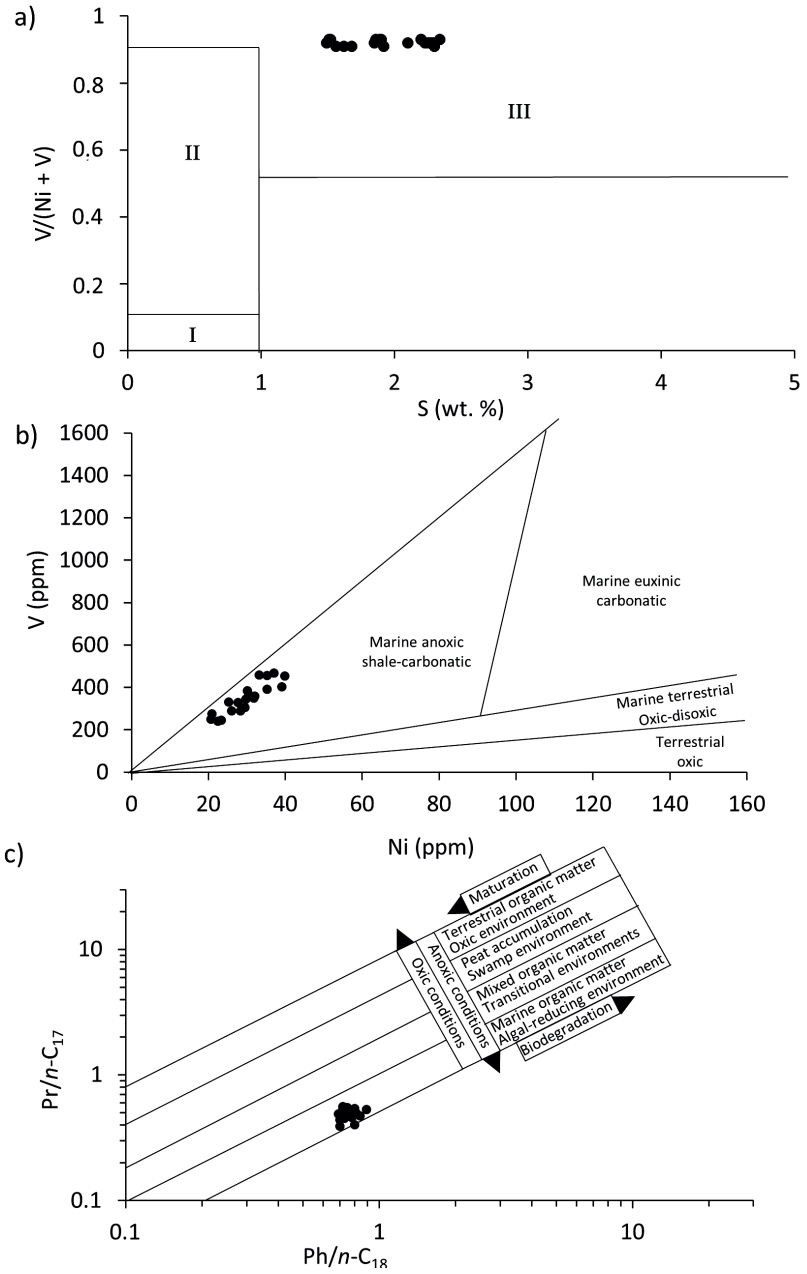

Fig. 10. Plots of: (a) sulphur content versus V/(Ni+V) (after Lewan, 1984); (b) Ni concentration (ppm) versus V concentration (ppm) (after Galarraga *et al.*, 2008); and (c) Ph/*n*-C_{18} versus Pr/*n*-C_{17} (after Shanmugam, 1985) for the analysed oils from the Río Negro Formation reservoir in the Urdaneta West field. Zones in Fig. 10a are: I, terrestrial oxic; II, marine-terrestrial dysoxic-suboxic; and III, carbonate marine anoxic.

the Pr/Ph ratios of <1 and Pr/*n*-C_{17} <0.5, the absence of oleananes and diahopanes (both of which were detected in Machiques Member extracts), as well as the distribution pattern of regular steranes ($C_{27} > C_{28} > C_{29}$), triterpenoid ratios (e.g. Ts/Tm values < 0.5) and the predominance of C_{23} cheilanthane over its counterparts (Figs 9a and 9b in Escobar *et al.*, 2011), it appears that the oil samples analysed show a good correlation with extracts of the La Luna Formation source rock.

The oil samples from the Río Negro reservoir show reliable sterane isomerization parameters (%20S and %ββ; Peters *et al.*, 2005) of 47-54% and 50-62% respectively (Table 3), which indicate a thermal maturity level at the onset of the oil window equivalent to a vitrinite reflectance (%R_o) of about 0.8% for kerogen Type II source rocks. In addition, %20S and %ββ values increase in samples from wells in the south of the Urdaneta West field, thereby suggesting a north-to-south oil maturity trend (Table 3 and Fig. 4). Such a trend is supported by a north-to-south increase in sample Ts/Tm and cheilanthane ratios (Table 3). Note that the Ts/Tm ratio is both a source- and maturity-related indicator (Moldowan *et al.*, 1986) but that it begins to increase at maturities in the peak oil window or above (van Grass, 1990). By contrast, ratios such as the sum of C_{23} and C_{24} tricyclic terpanes

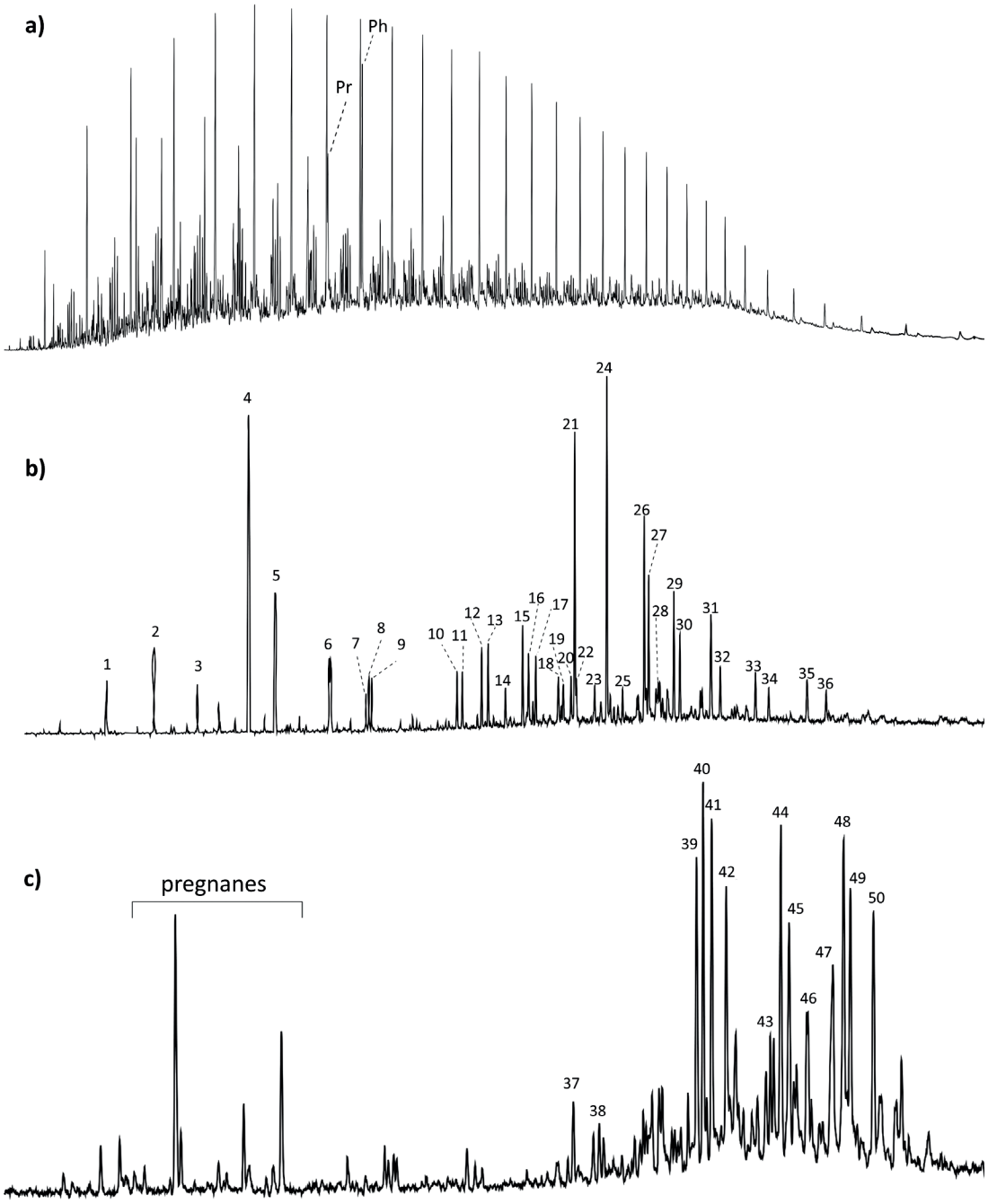

Fig. 11. Total ion current (TIC) (a), *m*/z 191 (b), and *m*/z 217 (c) ion chromatograms showing the *n*-alkane/isoprenoid, triterpane and sterane distributions, respectively, for saturates in a representative oil sample from the Río Negro reservoir in the Urdaneta West field. Peak identifications in the Appendix (page 302).

to the sum of C_{29} and C_{30} hopanes increase only as a result of maturation, probably due to a rearrangement of hopanoid compounds (Aquino Neto *et al.*, 1983).

These observations are consistent with the increasing API gravities and increasing proportions of saturated hydrocarbons for samples from wells in the south of the Urdaneta West field, along with decreasing sulphur contents (see Tables 2 and 3). This is probably due to a decrease in the proportion of polar compounds (resins plus asphaltenes) in the more mature oils which have accumulated in the southern part of the field (c.f. Tissot and Welte, 1984), as discussed below.

DISCUSSION

Characteristics of the La Luna/Río Negro(.) petroleum system

Key elements of the La Luna/Río Negro(.) petroleum system in oil-generation phases 1 and 2 are: the source rocks comprise limestones and calcareous shales in the La Luna Formation; reservoir rocks are sandstones in the Río Negro Formation; shales in the Colon Formation serve as the seal; and the Colon Formation and younger units constitute the overburden (Fig. 9). According to Talukdar and Marcano (1994),

this system extended over a time period of about 120 Ma from the deposition of the Río Negro Formation sandstones in the Early Cretaceous to hydrocarbon migration and accumulation during the late Neogene and Quaternary. Trap formation took place during structural deformation in the Paleocene and Eocene.

Slight differences in composition (e.g. the sulphur and polar contents), physical properties (e.g. API gravity) and levels of thermal maturity of the oils analysed from Urdaneta West, together with the fact that the thermal maturity of the La Luna Formation varies from north to south over the centre-west of the Lake Maracaibo Basin (Talukdar *et al.*, 1986), suggest that mixing of different oil charges appears to have taken place in the Río Negro reservoir. Both oil charges likely originated from the La Luna Formation but were generated at different times and at different maturity levels. Because both oil phases originated from the same source rock, their compositions are similar but are not identical.

Hydrocarbons appeared to have been generated during two phases: in the middle-late Eocene (phase 1) and in the Miocene to Holocene (phase 2). These two phases were associated with episodes of subsidence and burial which provided sufficient overburden for maturation of the La Luna Formation source rock to occur (e.g. Blaser and White, 1984) (Fig. 5). The thermal and burial history plots of the La Luna Formation in Fig. 5 indicate that phase 2 generation is continuing at the present day.

Reservoir-filling directions in the Urdaneta West field

Lateral variations in oil composition within a reservoir have been used to elucidate field-filling directions (e.g. Horstad and Larter, 1997) and may be related to the occurrence of successive petroleum charges (Horstad *et al.*, 1995). England *et al.* (1995) modelled density-driven mixing and homogenization of petroleum charges in a 2 km long and 100 m thick reservoir with good permeability (100 mD) and without evident transmissibility barriers. Their results indicate that mixing can be efficient within a reasonable geological timeframe (2 Ma). However, the Río Negro reservoir in the Urdaneta West field has lower permeability (0.2-15.0 mD) and is longer (11 km) and thinner (18 m) than that modelled by England *et al.* (1995). Therefore it may have been more difficult for hydrocarbon fluids to reach homogeneity within the studied reservoir (Márquez *et al.*, 2013).

It is assumed that the accumulation of more mature petroleum occurred in the reservoir as it was filled from a progressively subsiding and maturing source rock, and that the most mature oils would therefore be located nearest to the source rock kitchen or probable filling point (c.f. Tissot and Welte, 1984). In this regard, secondary south-to-north oil and gas migration to the Urdaneta West field can be inferred from a consideration of lateral variations in selected geochemical parameters (API gravity, sulphur and polar contents, and sterane isomerization ratios; see Fig. 4 and Table 2) in oils from the Río Negro Formation. These variations suggest that the Río Negro reservoir at Urdaneta West appears to have been filled from the south.

To investigate this migration model further, the thermal maturity of La Luna Formation cuttings samples from wells H and W (locations in Fig 1C and 4) were investigated (Ascue, 2007). Measured vitrinite reflectance values (0.6 $\%R_o$ on average) for cuttings of the formation from well H are lower than values for cuttings from well W to the south ($\%R_o \geq 0.8$). In addition, well W cuttings have thermal maturities similar to those calculated for the oils analysed, especially for those produced from the south of the field where the La Luna source rock is more deeply buried (Fig. 2a). These observations together with previous studies (Márquez *et al.*, 2013) suggest that secondary migration of hydrocarbons occurred during phase 2 generation from La Luna Formation source kitchens located to the south of the Urdaneta West field to Cretaceous reservoirs in the study area (Fig. 12). This contrasts with the first episode of petroleum migration during the Eocene from the La Luna source kitchen to Cretaceous reservoirs in the Urdaneta West field, which followed a general northeast to southwest direction (Blaser and White, 1984). These results can be explained by the existence of source kitchen areas to the south of the Urdaneta West field, where the La Luna Formation source rocks entered the oil window in the Miocene (Talukdar *et al.*, 1986), and the fact that these latter kitchens are responsible for most of the present-day oil which has accumulated in the field (Talukdar and Marcano, 1994).

Thus, as shown in Fig. 12, oil migrated during the middle-late Eocene (phase 1 generation) from a kitchen area to the north and NE of the Urdaneta West field in which the La Luna Formation was at an early stage of thermal maturity. More mature oil was generated and expelled from the same source rock during the late Miocene – Recent (phase 2 generation), and migration occurred from a hydrocarbon generating kitchen area to the south of the field.

Previous studies (e.g. Escobar *et al.*, 2012) have established that the Paleocene Marcelina and Eocene Misoa reservoir units in the Alturitas and Boscán fields (locations in Fig. 1), and in other oilfields located along the western coast of Lake Maracaibo, were filled from the south with a single pulse of petroleum migration from thermally mature La Luna source rocks. In all these cases, a Miocene to Recent La Luna Formation kitchen was proposed as the probable source of the

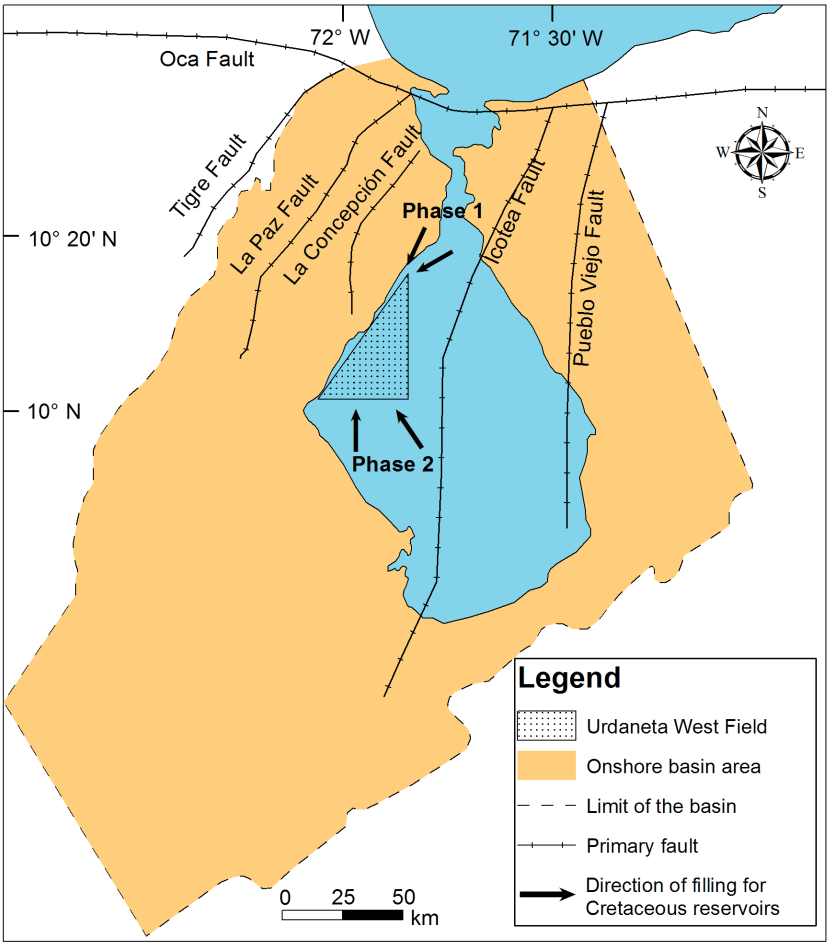

Fig. 12. Map showing the directions of secondary migration into the Cretaceous Río Negro Formation reservoir at Urdaneta West field, together with major regional faults (adapted from Escobar, 1987).

hydrocarbons (Escobar, 1987). The oils produced from these latter reservoirs exhibit a progressive increase in polar contents towards the south, as opposed to the trend observed for the oil samples from the Río Negro reservoir in the Urdaneta West field. These apparently contradictory results can be interpreted as indicative of a geochromatographic effect during the migration of oil which has accumulated in the Marcelina and Misoa reservoirs (c.f. Larter *et al.*, 2000) along a preferential south-north axis. By contrast, oils from the Río Negro reservoir at Urdaneta West show sterane isomerization ratios (Table 3) that would plot to the left of a graph of %20S versus %ββ proposed by Seifert and Moldowan (1986), and a geochromatographic effect during long-distance secondary migration can therefore be precluded in this case (Peters *et al.*, 2005).

CONCLUSIONS

Burial and thermal history reconstructions for wells X, Y and Z in the Offshore Urdaneta District in the north of the Urdaneta West field (Lake Maracaibo Basin, NW Venezuela) show that the Upper Cretaceous La Luna Formation source rock has been buried sufficiently deeply to become early to late mature for oil and gas generation. A main stage of hydrocarbon generation and expulsion occurred during the Eocene with a second, much smaller phase during the Neogene – Quaternary.

Modelled values of the transformation ratio for the La Luna source rock at wells X, Y and Z reached 35%, 98% and 100% by the end of the Eocene. The high transformation ratios for the main (Eocene) oil generation phase from the La Luna Formation in wells Y and Z, compared with that for well X, could be explained by the lower geothermal gradient in the well X location.

Biomarker-based oil-source correlations confirm that samples of produced oils from the Río Negro reservoir in the Urdaneta West field originated from the La Luna source rock. Based on lateral variations in bulk geochemical and biomarker data for oil samples from the Río Negro reservoir, a north-to-south south compositional gradient was observed in the field, suggesting that successive charges of increasingly more mature hydrocarbon fluids migrated into the reservoir. The more mature hydrocarbons appear to have migrated from a La Luna Formation source

kitchen located to the south of the Urdaneta West field where petroleum generation and expulsion took place in the Neogene – Quaternary.

ACKNOWLEDGEMENTS

J.G. Diaz acknowledges the support of the PDVSA Western Exploration Project Management and the University of Zulia. The authors are grateful to Iván Chirino and Patricia Marín for their scientific assistance. We are also grateful to the JPG referees (Karla Quintero-Bonilla, Katya Reategui and anonymous) whose comments helped to improve the original version of this manuscript. Carlos Boente obtained a post-doctoral contract within the program PAIDI 2020 (Ref 707 DOC 01097), co-financed by the Junta de Andalucía (Andalusian Government) and the EU.

Data availability statement

Data is available from the corresponding author on reasonable request.

REFERENCES

ALBERDI-GENOLET, M. and TOCCO, R., 1999. Trace metals and organic geochemistry of the Machiques Member (Aptian-Albian) and La Luna Formation (Cenomanian-Campanian), Venezuela. *Chem. Geol.*, **160**, 19-38. https://doi.org/10.1016/S0009-2541(99)00044-3

ALLEN, P. and ALLEN, J., 2005. Basin Analysis, Principles and Applications, 2nd Edition. Blackwell Publishing, Oxford, 549 pp.

AQUINO NETO, F., TRENDEL, J., RETLE, A., CONNAN, J. and ALBRECHT, P., 1983. Occurrence and formation of tricyclic and tetracyclic terpanes in sediments and petroleums. In: BJORØY, M., ALBRECHT, C., BLASER, R. and WHITE, C., 1984. Source rock and carbonization study, Maracaibo Basin, Venezuela. In: DEMAISON, G. and MURRIS, R.J. (Eds), Petroleum Geochemistry and Basin Evaluation. *AAPG Memoir* **35**, 229-252.

ASCUE, C. A., 2007. Application of geochemical and physicochemical parameters for oil-source rock correlation: La Luna Formation-Centro Lago crude oils. MSc. Thesis, Central University of Venezuela, Caracas, 161 pp.

ASHRAFI, T., SABERI, M. H., ZARENEZHAD, B., 2020. 1D and 2D basin modeling, in evaluating the hydrocarbon generation-migration-accumulation potential, at coastal Fars Area, Southern Iran. *Journ. Petrol. Sci. Eng.,* **195**, 107594.

BASKIN, D.K, 1997. Atomic H/C Ratio of Kerogen as an Estimate of Thermal Maturity and Organic Matter Conversion. *AAPG Bulletin*, **81**, 1437-1450. https://doi: 10.1306/3B05BB14-172A-11D7-8645000102C1865D

BLASER, R. and WHITE, C., 1984. Source rock and carbonization study, Maracaibo Basin, Venezuela. In: Demaison, G. and Murris, R. J. (Eds), Petroleum Geochemistry and Basin Evaluation. *AAPG Memoir* **35**, 229-252. AAPG, Tulsa, USA.

BRACHO, E.E., 2010. Geochemistry of Cretaceous oils from Lake Maracaibo Basin. MSc. Thesis, University of Zulia, Maracaibo, 187 pp.

BURNHAM, A.K. and BRAUN, R.L., 1990. Development of a detailed model of petroleum formation, destruction, and expulsion from lacustrine and marine source rocks. In: DURAND, B. and BEHAR, E (Eds), Advances in Organic Geochemistry 1989. Pergamon Press, Oxford, pp 27-39.

CORNFORD, C., DE GROOT, K., EGLINTON, G., GALIMOV, E., LEYTHAEUSER, D.D., PELET, R., RULLKÖTTER, J. and SPEERS, G. (Eds), 1981. Advances in Organic Geochemistry 1981. Wiley, New York, pp. 659-676.

DÍAZ, J., 2018. 1D and 2D Basin Modeling of hydrocarbon generation, expulsion and migration from the La Luna formation in the Urdaneta West Field, Lake Maracaibo Basin. MSc. Thesis, University of Zulia, Maracaibo, 263 pp.

DZOU, L., HOLBA, A., RAMÓN, J. MOLDOWAN, J.M. and ZINNIKER, D., 1999. Application to new diterpane biomarker to source, biodegradation and mixing effects on central Llanos Basin oils, Colombia. *Org. Geochem.*, **30**, 515–534.

ENGLAND, W.A., MUGGERIDGE, A., CLIFFORD, P. and TANG, Z., 1995. Modeling density-driven mixing rates in petroleum reservoirs on geological time-scales, with application to the detection of barriers in the Forties Field (UKCS). In: CUBITT, J. and ENGLAND, W. (Eds), The Geochemistry of Reservoirs. *Geol. Soc. London, Special Publication* **86**, 185-201. https://doi: 10.1144/gsl.sp.1995.086.01.13

ESCALONA, A. and MANN, P., 2006. An overview of the petroleum system of Maracaibo Basin. *AAPG Bulletin*, **90**, 653-674. https://doi.:10.1306/10140505038

ESCALONA, A. and MANN, P., 2011. Tectonics, basin subsidence mechanisms, and paleogeography of the Caribbean-South American plate boundary zone. *Mar. Petrol. Geol.*, **28**, 8-39.

ESCOBAR, M., 1987. Petroleum Geochemistry at the North-Central Region of the Western Coast of the Maracaibo Lake, Venezuela. PhD Thesis, Central University of Venezuela, Caracas, 396 pp.

ESCOBAR, M., MÁRQUEZ, G., INCIARTE, S., ROJAS, J., ESTEVES, I., MALANDRINO, G., 2011. The organic geochemistry of oil seeps from the Sierra de Perijá eastern foothills, Lake Maracaibo Basin, Venezuela. *Org. Geochem.*, **42**, 727-738.

ESCOBAR, M., MÁRQUEZ, G., SUÁREZ-RUIZ, I., JULIAO, T.M., CARRUYO, G. and MARTÍNEZ, M., 2016. Source-rock potential of the lowest coal seams of the Marcelina Formation at the Paso Diablo mine in the Venezuelan Guasare Basin: Evidence for the correlation of Amana oils with these Paleocene coals. *Int. Journ. Coal Geol.*, **163**, 149-165. doi.org/10.1016/j.coal.2016.07.003

ESQUINAS, N., MÁRQUEZ, G., PERMANYER, A., and GALLEGO. J.R., 2018. Geochemical evaluation of crude oils from the Caracara and Tiple areas, Eastern Llanos Basin, Colombia: Palaeo biodegradation and oil mixing. *Journal of Petroleum Geology*, **41**, 113–134.

GALARRAGA, F., REATEGUI, K., MARTÍNEZ, A., MARTÍNEZ, M., LLAMAS, J.F., MÁRQUEZ, G., 2008. V/Ni ratio as a parameter in palaeoenvironmental characterisation of non-mature medium-crude oils from several Latin American basins. *Journ. Petrol. Sci. Eng.*, **61**, 9-14.

GALARRAGA, F., URBANI, F., ESCOBAR, M., MÁRQUEZ, M., MARTÍNEZ, M. and TOCCO, R., 2010. Main factors controlling the compositional variability of the oil seeps from Trujillo State, western Venezuela. *Journal of Petroleum Geology*, **33**, 255–268.

GRANTHAM, P.J. and WAKEFIELD, L.L., 1988. Variations in the sterane carbon number distributions of marine source rocks derived crude oils through geological time. *Org. Geochem.*, **12**, 61-73.

GUZMÁN, J.I. and FISHER, W.L., 2006. Early and middle Miocene depositional history of the Maracaibo Basin, western Venezuela. *AAPG Bull.*, **90**, 625-655. doi:10.1306/10110505035

HAKIMI, M.H., ABDULLAH, W.H. and SHALABY, M.R., 2010. Organic geochemistry, burial history and hydrocarbon generation modelling of the Upper Jurassic Madbi Formation, Masila Basin, Yemen. *Journal of Petroleum Geology*, **33**, 299–318.

HANTSCHEL, T. and KAUERAUF, A., 2009. Fundamentals of Basin and Petroleum Systems Modeling. Springer, Heidelberg

(Germany), 436 pp.
HORSTAD, I. and LARTER, S., 1997. Petroleum migration, alteration, and re-migration within the Troll Field, Norwegian North Sea. *AAPG Bulletin*, **81**, 222-248.
HORSTAD, I., LARTER, S. and MILLS, N., 1995. Migration of hydrocarbons in the Tampen Spur area, Norwegian North Sea: A reservoir geochemical evaluation. In: Cubitt J. and England W. (Eds.): The Geochemistry of Reservoirs. *Geol Soc. London, Special Publication* **86,** 159-183. doi:10.1144/gsl.sp.1995.086.01.12.
JAMES, K.H., 2000. The Venezuelan hydrocarbon habitat, part 2: Hydrocarbon occurrences and generated-accumulated volumes. *Journal of Petroleum Geology,* **23**, 133-164. doi: 10.1111/j.1747-5457.2000.tb00488.x
KLEMME, H.D., 1975. Geothermal gradients, heat flow and hydrocarbon recovery. In: Fischer, A.G. and Judson, S. (Eds.): Petroleum and Global Tectonics. Princeton University Press, New Jersey, 251-304.
KRAUSE, H.H. and JAMES, K.H., 1990. Hydrocarbon resources of Venezuela, their source rocks and structural habitat. In: ERICKSEN, G.E., CAÑAS, M.T. and REINEMUND, J.A. (Eds.): Circum-Pacific Council for Energy and Mineral Resources. *Earth Science Series*, **11**, Houston, 405-414.
LARTER, S., BOWLER, B., CLARKE, E., YARDLEY G., WILSON, C., MOFFATT, B., BENNETT, B. and CARRUTHERS, D., 2000. An experimental investigation of geochromatography during secondary migration of petroleum performed under subsurface conditions with a real rock. *Geochem. Transact.*, **1**, 54-61. doi:10.1039/b006737g
LEWAN, M.D., 1984. Factors controlling the proportionality of vanadium to nickel in crude oils. *Geochim. Cosmochim. Acta*, **48**, 2231-2238.
LEWAN, M.D. and MAYNARD, J.B., 1982. Factors controlling enrichment of vanadium and nickel in the bitumen of organic sedimentary rocks. *Geochim. Cosmochim. Acta*, **46**, 2547-2560.
LUGO, J. and MANN, P., 1995. Jurassic – Eocene tectonic evolution of Maracaibo Basin, Venezuela. In: TANKARD, A. J., SUÁREZ, S. and WELSINK, H.J. (Eds), Petroleum Basins of South America. *AAPG Memoir* **62**, 699-726.
MACELLARI, C.E., 1988. Cretaceous paleogeography and depositional cycles of western South America. *Journ. South Am. Earth Sci.*, **1**, 373-418.
MAGOON, L.B. and DOW, W.G., 1994. The petroleum system. In: MAGOON, L.B. and DOW, W. G., (Eds), The Petroleum System - from Source to Trap. *AAPG Memoir*, **60**, 3-24.
MANN, P., ESCALONA, A. and CASTILLO, M.V., 2006. Regional geologic and tectonic setting of the Maracaibo supergiant basin, western Venezuela. *AAPG Bulletin*, **90**, 445-477. doi: 10.1306/10110505031
MÁRQUEZ, G., ESCOBAR, M,. LORENZO, E., GALLEGO, J.R. and TOCCO, R., 2013. Using gas geochemistry to delineate structural compartments and assess petroleum reservoir-filling directions: A Venezuelan case study. *Journ. South Am. Earth Sci.*, **43**, 1-7.
MOLDOWAN, J.M., SUNDARARAMAN, P. and SCHOELL, M., 1986. Sensitivity of biomarker properties to depositional environment and/or source input in the Lower Toarcian of SW-Germany. *Org. Geochem.*, **10**, 915-926.
MONDAL, D., SARKAR, K., ISLAM, M.S., SANG, S., MOSTAFA, M.G., 2021. Evaluation of petroleum system using 1D modeling technique of well Atgram-1X, Zakiganj, Bengal Basin. *Arab. Journ. Geosci.* **14**, 2803.
MONTILLA, O.J., 2018. Structural model of the Cretaceous sequence in the western coast of Lake Maracaibo. MSc. Thesis, University of Zulia, Maracaibo, 119 pp.
NIELSEN, S.B., CLAUSEN, O.R. and McGREGOR, E., 2015. Basin%Ro: A vitrinite reflectance model derived from basin and laboratory data. *Basin Research*, **29**, 515-536. doi:10.1111/bre.12160.
PÉREZ-INFANTE, J., FARRIMOND, P. and FURRER, M., 1996. Global and local controls influencing the deposition of the La Luna Formation Cenomanian – Campanian, western Venezuela. *Chem. Geol.* **130**, 271-288. doi.org/10.1016/0009-2541(96)00019-8
PETERS, K.E. and MOLDOWAN, J. M., 1991. Effects of source, thermal maturity, and biodegradation on the distribution and isomerization of homohopanes in petroleum. *Org. Geochem.*, **17**, 47-61.
PETERS, K.E., SCHENK, O., HOSFORD-SCHEIRER, A., WYGRALA, B. and HANTSCHEL, T., 2017. Basin and petroleum system modeling. In: Hsu, C.S. and Robinson, P.R. (Eds), Handbook of Petroleum Technology. Springer, Berlin, 381-417. doi 10.1007/978-3-319-49347-3_11
PETERS, K.E., WALTERS, C. and MOLDOWAN, J., 2005. The Biomarker Guide: Biomarkers and Isotopes in Petroleum Systems and Earth history, 2nd edition. Cambridge University Press, Cambridge, 1132 pp.
PÖPPELREITER, M., BALZARINI, M., DE SOUSA, P., ENGEL, S., GALARRAGA, M., HANSEN, B., MÁRQUEZ, X., MORELL, J., NELSON, R. and RODRÍGUEZ, F., 2005. Structural control on sweet-spot distribution in a carbonate reservoir: Concepts and 3-D models (Cogollo Group, Lower Cretaceous, Venezuela). *AAPG Bulletin*, **89**, 1651-1676. doi:10.1306/08080504126
RULLKÖTTER, J., SPIRO, B. and NISSENBAUM, A., 1985. Biological marker characteristics of oils and asphalts from carbonate source rocks in a rapidly subsiding graben, Dead Sea, Israel. *Geochim. Cosmochim. Acta*, **49**, 1357-1370.
SÁNCHEZ, L.A., 2013. Analysis and interpretation of pressure buildup tests carried out in wells completed in the RNG UD-106 reservoir within the Urdaneta Oeste Field. MSc. Thesis, Central University of Venezuela, Caracas, 205 pp.
SEIFERT, W.K. and MOLDOWAN, J.M., 1986. Use of biological markers in petroleum exploration. In: R.B. Johns (Ed.), *Methods in Geochemistry and Geophysics* **24**. Elsevier, Amsterdam, pp 261-290.
SHANMUGAM, G., 1985. Significance of coniferous rain forests and related organic matter in generating commercial quantities of oil, Gippsland Basin, Australia. *AAPG Bulletin*, **69**, 1241-1254.
SWEENEY, J.J., BRAUN, R.L., BURNHAM, A.K., TALUKDAR, S. and VALLEJOS, C., 1995. Chemical kinetic model of hydrocarbon generation, expulsion, and destruction applied to the Maracaibo Basin, Venezuela. *AAPG Bulletin*, **79**, 1515-1532.
TALUKDAR, S. and MARCANO, F., 1994. Petroleum system of the Maracaibo Basin, Venezuela. In: MAGOON, L.B. and DOW, W.G. (Eds), The Petroleum System – from Source to Trap. *AAPG Memoir*, **60**, 463-482.
TALUKDAR, S., GALLANGO, O. and CHIN-A-LIEN, M., 1986. Generation and migration of hydrocarbon in the Maracaibo Basin, Venezuela: An integrated basin study. *Org. Geochem.*, **10**, 261-279. doi.org/10.1016/0146-6380(86)90028-8
TISSOT, B. P. and WELTE, D. H., 1984. Petroleum formation and occurrence, 2nd Edition. Springer-Verlag, New York, 699 pp.
VAN GRAAS, G.W., 1990. Biomarker maturity parameters for high maturities: calibration of the working range up to the oil/condensate threshold. *Org. Geochem.*, **16**, 1025-1032.
VAN KAAM-PETERS, H.M.E., KÖSTTER, J., VAN DER GAAST, S.J., DEKKER, M., DE LEEUW, J.W. and SINNINGHE DAMSTÉ, J.S., 1998. The effect of clay minerals on diasterane/sterane ratios. *Geochim. Cosmochim. Acta,* **62**, 2923-2929.
VILLAMIL, T., 1999. Campanian–Miocene tectonostratigraphy, depocenter evolution and basin development of Colombia and western Venezuela. *Palaeogeogr. Palaeoclimatol. Palaeoecol.*, **153**, 239-275. doi.org/10.1016/S0031-0182(99)00075-9
VILLAMIL, T. and PINDELL, J. L., 1998. Mesozoic paleogeographic evolution of northern South America: Foundation for sequence stratigraphic studies in passive margin strata

deposited during non-glacial times. In: PINDELL, J.L. and DRAKE, C. (Eds), Paleogeographic evolution and non-glacial eustasy in North America. *SEPM Special Publication*, **58**, 283-318.

VOLKMAN, J.K. and MAXWELL, J.R., 1986. Acyclic isoprenoids as biological markers. In: R.B. Johns (Ed.), Biological markers in the sedimentary record. Elsevier, New York, 1-42.

WAPLES, D.W., KAMATA, H. and SUIZU, M., 1992. The art of maturity modeling, part 1, finding a satisfactory geologic model. *AAPG Bulletin,* **76**, 31-46.

WENGER, L.M., DAVIS, C.L. and ISAKSEN, G.H., 2002. Multiple controls on petroleum biodegradation and impact on oil quality. *SPE Reserv. Eval. Eng.*, **5**, 375-383.

YALCIN, M. N., LITTKE, R. and SACHSENHOFER, R. F., 1997. Thermal history of sedimentary basins. In: Welte, D.H., Horsfield, B., Baker, D.R. (Eds), Petroleum and Basin Evolution. Springer, Berlin, 71-167.

Appendix. Main saturated biomarkers identified in the mass chromatograms.

1	C_{20}-Tricyclic terpane	26	17α(H),21β(H)-29-Homohopane 22S
2	C_{21}-Tricyclic terpane	27	17α(H),21β(H)-29-Homohopane 22R
3	C_{22}-Tricyclic terpane	28	17β(H),21α(H)-29-Homomoretane 22S+22R
4	C_{23}-Tricyclic terpane	29	17α(H),21β(H)-29-Bishomohopane 22S
5	C_{24}-Tricyclic terpane	30	17α(H),21β(H)-29-Bishomohopane 22R
6	C_{25}-Tricyclic terpane 17R+17S	31	17α(H),21β(H)-29-Trishomohopane 22S
7	C_{24}-17,21-secohopane	32	17α(H),21β(H)-29-Trishomohopane 22R
8	C_{26}-Tricyclic terpane 17R	33	17α(H),21β(H)-29-Tetrahomohopane 22S
9	C_{26}-Tricyclic terpane 17S	34	17α(H),21β(H)-29-Tetrahomohopane 22R
10	C_{28}-Tricyclic terpane 17R	35	17α(H),21β(H)-29-Pentahomohopane 22S
11	C_{28}-Tricyclic terpane 17S	36	17α(H),21β(H)-29-Pentahomohopane 22R
12	C_{29}-Tricyclic terpane 17R	37	13β(H),17α(H)-Diacholestane 20S
13	C_{29}-Tricyclic terpane 17S	38	13β(H),17α(H)-Diacholestane 20R
14	18α(H)-22,29,30-Trisnorneohopane	39	5α(H),14α(H),17α(H)-Cholestane 20S*
15	17α(H)-22,29,30-Trisnorhopane	40	5α(H),14β(H),17β(H)-Cholestane 20R*
16	C_{30}-Tricyclic terpane 17R	41	5α(H),14 β(H),17β(H)-Cholestane 20S
17	C_{30}-Tricyclic terpane 17S	42	5α(H),14α(H),17α(H)-Cholestane 20R
18	17α(H),21β(H)-28,30-Bisnorhopane	43	5α(H),14α(H),17α(H)-Ergostane 20S
19	17β(H),21α(H)-28,30-Bisnorhopane	44	5α(H),14β(H),17β(H)-Ergostane 20R*
20	C(14α)-Homo-26-nor-17α(H)-hopane?	45	5α(H),14β(H),17β(H)-Ergostane 20S
21	17α(H),21β(H)-30-Norhopane	46	5α(H),14α(H),17α(H)-Ergostane 20R
22	18α(H)-30-Norneohopane	47	5α(H),14α(H),17α(H)-Stigmastane 20S
23	17β(H),21α(H)-30-Normoretane	48	5α(H),14β(H),17β(H)-Stigmastane 20R
24	17α(H),21β(H)-Hopane	49	5α(H),14β(H),17β(H)-Stigmastane 20S
25	17β(H),21α(H)-Moretane	50	5α(H),14α(H),17α(H)-Stigmastane 20R

*Peak co-elution